BRITISH ANTARCTIC SURVEY
SCIENTIFIC REPORTS
No. 55

SEISMIC REFRACTION INVESTIGATIONS IN THE SCOTIA SEA

By
A. ALLEN, M.Sc., Ph.D.
British Antarctic Survey
and
Department of Geology, University of Birmingham

LONDON: PUBLISHED BY THE BRITISH ANTARCTIC SURVEY: 1966

BRITISH ANTARCTIC SURVEY SCIENTIFIC REPORTS: No. 55

SEISMIC REFRACTION INVESTIGATIONS IN THE SCOTIA SEA

By

A. ALLEN, M.Sc., Ph.D.

British Antarctic Survey
and
Department of Geology, University of Birmingham

(Manuscript received 14th September, 1965)

ABSTRACT

DURING December 1962 seismic refraction investigations of the east Scotia Sea were undertaken by the Department of Geology, University of Birmingham, in collaboration with the British Antarctic Survey and the Royal Navy. The seismic survey formed part of a series of gravity, magnetic and seismic investigations of the Scotia Sea, the Scotia Ridge and the Antarctic Peninsula which began in 1959.

The seismic refraction survey described in this report comprises one unreversed and nine reversed lines which were shot in profile across the Scotia Sea from the South Orkney Islands to South Georgia. Interpretation of the results of the seismic survey has been hampered by poor-quality information on the velocities of the shallow refractors on and below the sea bed. The methods of obtaining the velocities of the sea-bed sediments from sea-bottom reflection data are discussed, and a new method which uses the ratio between the amplitudes of the first- and second-order sea-bottom reflections is suggested, although it is appreciated that the full advantages of this method may only be realized with improved recording techniques. The results of the seismic survey show that the south-eastern parts of the Scotia Sea have a lower- or sub-crustal velocity of about 7·5 km./sec., whilst the northern parts to the west of South Georgia have a sub-crustal velocity of 8·0 km./sec. Crustal velocities in the Scotia Sea average about 6·0 km./sec.

Current theories on the origin of the Scotia island arc are discussed, and it is suggested that the inconsistencies in these theories necessitate an explanation of the evolution of the whole region in terms of continental drift between South America and Antarctica. It is suggested that an explanation in these terms would be consistent with the indications of different seismicities of the northern and southern parts of the Scotia Ridge, and with the anomalous trends of the foliation axes in the basement rocks of the South Orkney Islands. According to this theory, the Scotia Ridge should be viewed as a late Palaeozoic–Triassic mountain or cordilleran arc, which has been ruptured between South Georgia and the South Orkney Islands, and between the South Shetland and South Orkney Islands. It is generally believed that the South Sandwich Islands group is not fundamentally related to the older islands of the Scotia Ridge or to the Andean orogenic belt of this region, but it is suggested that the continuity of this orogenic belt is preserved in a submarine volcanic arc to the west of the South Sandwich Islands group which may extend from South Georgia to the South Orkney Islands. The similarities between the Scotia and Caribbean island arcs are discussed and it is suggested that theories developed to explain the seismic results obtained in the Venezuelan Basin may be directly applicable to those obtained in the south-eastern Scotia Sea.

CONTENTS

I. INTRODUCTION

DURING December 1962 one unreversed and nine reversed seismic refraction lines were shot along a profile across the Scotia Sea from the South Orkney Islands to South Georgia. This work was achieved by collaboration between the Department of Geology, University of Birmingham, the British Antarctic Survey and the Royal Navy. Personnel from the University of Birmingham and the British Antarctic Survey were responsible for the technical aspects of the survey; R.R.S. *Shackleton* (British Antarctic Survey) acted as receiving ship and H.M.S. *Protector* (Royal Navy) acted as shooting ship.

The Scotia Sea (Fig. 1) is bounded on the north, east and south by the Scotia Ridge which is an almost continuous chain of submarine ridges and islands joining Tierra del Fuego in the north with the Antarctic

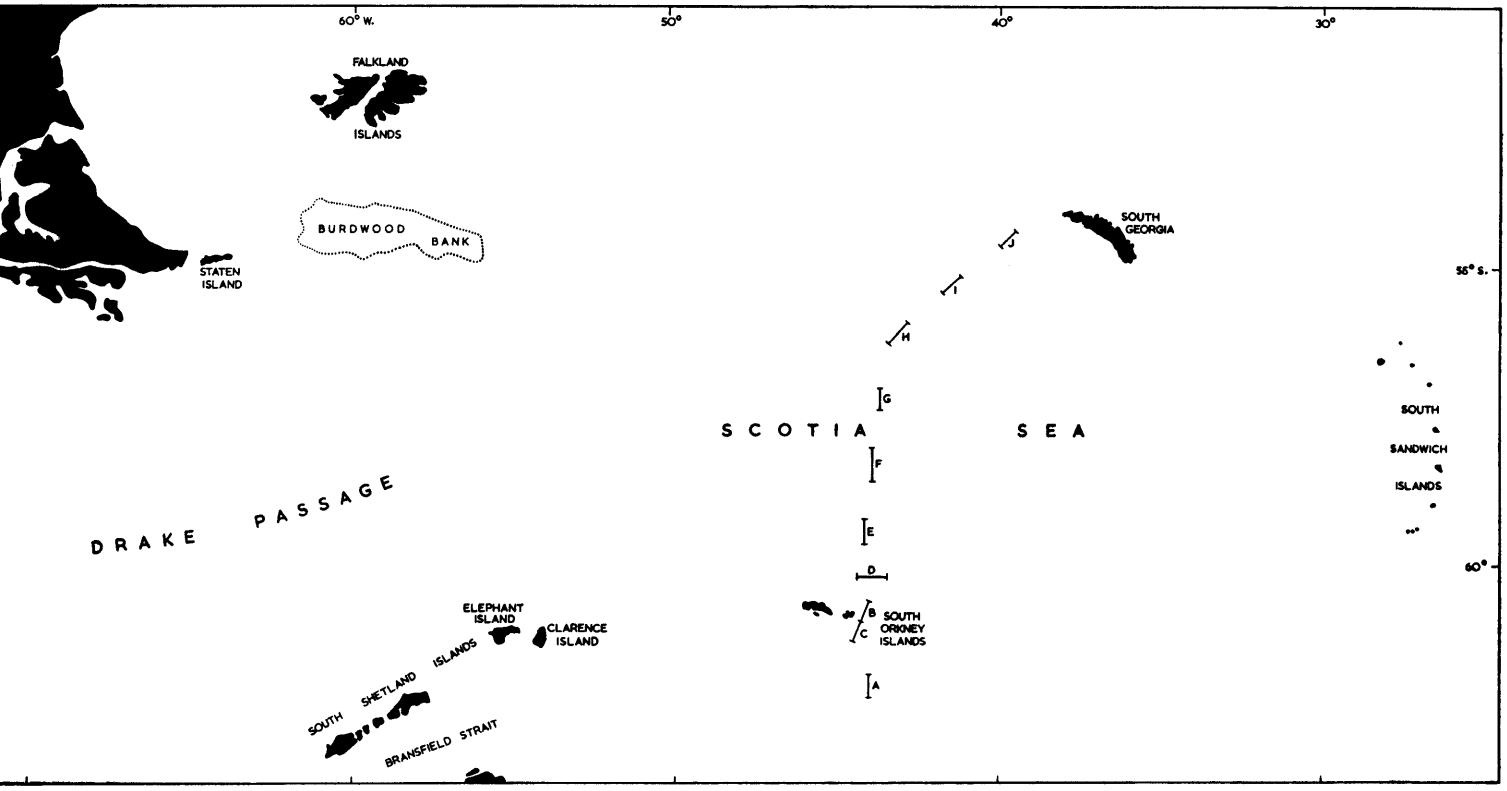

FIGURE 1

Sketch map of the Scotia Sea, showing the location of the seismic refraction profile between the South Orkney Islands and South Georgia.

Peninsula in the south. The complex of submarine ridges, islands and troughs (Plate I) has been designated the Scotia arc,* because of the features it has in common with other island arc structures. In particular, it has been compared with the Caribbean Arc, and the close parallelism of the physiographic, structural and seismological features of these two regions has been noted by Heezen and Johnson (1965), and others.

The area of survey, although necessarily selected for logistic reasons, was chosen because of the information it might yield on the broader aspects of the structure and geology of the Scotia Sea. It seemed particularly worthwhile to attempt an investigation which might have a direct bearing on the

* The term "Scotia Ridge" is used to describe the submarine ridge and islands which extend in an arc from Tierra del Fuego to the Antarctic Peninsula. Many authors have used the term "Scotia arc", since this emphasizes the similarity between the features of the Scotia Ridge and those of other island arcs. The author is aware of the advantages and implications of using the term "Scotia arc", but in this report the earlier accepted name, "Scotia Ridge", has been adhered to.

two opposing theories of the structural and geological nature of the Scotia Ridge and the Scotia Sea. Matthews (1959) has asserted that the islands of the Scotia arc are continental in character and he has suggested that the Scotia Sea is in the process of evolving from a continental to an oceanic character. Hawkes (1962) has proposed that the Scotia Ridge represents a dissected land bridge between Tierra del Fuego and the Antarctic Peninsula which has drifted eastwards. He has suggested that the oceanic crust of the Scotia Sea is slowly becoming continental in character.

Previous geophysical investigations

The seismic refraction profile from the South Orkney Islands to South Georgia intersects a profile completed by Ewing and Ewing (1959*a*) near South Georgia. Other profiles reported by Ewing and Ewing indicate a normal oceanic crust overlying a mantle with a velocity of 8·3 km./sec. in an area south of Tierra del Fuego and the Burdwood Bank (Woollard, 1960). Profiles across the Falkland Ridge and the Scotia Ridge east of the Falkland Islands gave velocities of 5·7 to 6·3 km./sec. for the crustal layer with no indication of the mantle (Ewing and Ewing, 1959*a*). These are lower than typical oceanic crustal velocities in an area where the water depth of about 3 km. is also less than the average oceanic depths of about 5 km. A particularly interesting sub-crustal velocity of 7·6 km./sec. has been recorded by Ewing and Ewing (1959*a*) in the Scotia Sea south of South Georgia. The seismic profile shown in Fig. 1 was completed in part to determine whether the anomalous sub-crustal velocity of 7·6 km./sec. is only confined to the area south of South Georgia or whether it is characteristic of the eastern areas of the Scotia Sea.

Routine magnetic investigations are being carried out over the whole of the Scotia Sea by the Department of Geology, University of Birmingham, in collaboration with the British Antarctic Survey. This research group has also completed a detailed seismic refraction investigation of the Bransfield Strait and a gravity survey of the islands comprising the Scotia Ridge and parts of the Antarctic Peninsula (Griffiths and others, 1964).

Although some of the sea magnetic investigations offer some substantiation of suggested geological features to the south and east of the Falkland Islands, the significance of most of the marine magnetic survey in relation to the present seismic investigations between the South Orkney Islands and South Georgia is not yet clear.

II. GEOLOGY

ACCOUNTS of the geology of the Antarctic Peninsula and the islands comprising the Scotia Ridge have been given by Holtedahl (1929), Barth and Holmsen (1939), Tyrrell (1945), Adie (1957*a*, *b*, 1958, 1962), Trendall (1953, 1959), Matthews (1959) and Hawkes (1962). Adie (1964) has given a comprehensive summary of the present state of geological knowledge of both the Antarctic Peninsula and the Scotia Ridge. It is therefore unnecessary to give a detailed account of the geology of this region here, but some geological features important for discussion of the interpretation of the seismic refraction survey are included. The geology of the more remote areas is discussed elsewhere (p. 39–40) in relation to the theories concerning the origin of the Scotia Ridge.

1. *South Georgia*

The geology of South Georgia has been described by Trendall (1953, 1959). There are two sedimentary units on the island:

i. *Sandebugten Series.* Trendall (1953) has shown that this series has close petrographic similarity to the greywackes of the South Orkney Islands and Graham Land. The Sandebugten Series is composed of quartzose greywackes and it has been severely folded about axes parallel to the length of the island. Small fragments of lava are present both in this series and in its correlatives in the South Orkney Islands and Graham Land.

ii. *Cumberland Bay Series.* This is the younger series, composed of tuffaceous greywackes in the lower part and interbedded spilitic rocks near the top of the succession. Rocks correlated with the uppermost part of the Cumberland Bay Series have yielded an Aptian fauna at Annenkov Island, south-west of South Georgia. The rocks of this series are not folded at

Annenkov Island but the intensity of folding increases towards the north-east of South Georgia. The sediments of the lower part of the Cumberland Bay Series could have been derived wholly from volcanic rocks.

Gordon (1930) has identified a small piece of fossil wood (*Dadoxylon* (*Araucarioxylon*)) in a loose block of tuff from the Cumberland Bay Series at the Bay of Isles. This gives the Cumberland Bay Series an age certainly not older than Carboniferous and probably not younger than Jurassic (Trendall, 1953, p. 3). At the south-eastern end of South Georgia there is a granite-gabbro intrusive complex, which has been given a tentative late Cretaceous—early Tertiary age, and huge xenoliths found in this complex are considered to have been derived from an underlying metamorphic basement (Trendall, 1959). Recent detailed mapping near Cumberland Bay has led to the conclusion that there is probably an unconformity between the Cumberland Bay and Sandebugten Series (Adie, 1964).

2. *South Sandwich Islands*

The South Sandwich Islands group is composed of ten Recent or active volcanic islands. The volcanic rocks have been described by Tyrrell (1945) as olivine-basalts, andesites and dacites, which have affinities closer to those of the Caribbean Arc than to the Recent volcanic rocks of the Andes.

3. *South Orkney Islands*

The Basement Complex, which crops out at the western end of the island group, is composed of substantial thicknesses of *para*-schists of garnet grade, dominantly quartz-mica-schists with subordinate *para*-amphibolites and marbles. The Greywacke-Shale Series has already been compared with similar rocks of South Georgia and Graham Land. A younger series exposed in the eastern part of the islands is a conglomerate group, which could be Cretaceous in age and has only slight indications of east—west folding. The Greywacke-Shale Series is intensely folded about axes trending north-north-west to south-south-east. Folding about similar axes also occurs in the Basement Complex. Significant east—west tear faulting has been inferred between Signy and Coronation Islands (Adie, 1964). The South Orkney Islands are separated from the Elephant and Clarence Islands group by a pronounced trough where the depth of the sea is 3,000 m.

4. *Elephant and Clarence Islands group*

Tilley (1935, p. 390) has suggested a connection between the metamorphic rocks of the Elephant and Clarence Islands group and those of the South Orkney Islands. Tyrrell (1945, p. 76–83) has described these as low-grade metamorphic rocks (garnet-hornblende-albite-schists, amphibole-bearing marbles and *para*-amphibolites), which are remarkably similar to the schists of the South Orkney Islands. However, the general strike of the foliation in the basement rocks of Elephant and Clarence Islands is parallel to the trend of the submarine ridge on which the South Shetland Islands lie.

5. *Graham Land*

The geological units, which are most important in the discussion on the interpretation of the seismic refraction results and the theories on the origin of the Scotia Ridge, are the Trinity Peninsula Series and the Andean Intrusive Suite. The highly folded Trinity Peninsula Series has been given a tentative age of Carboniferous. The Andean Intrusive Suite is widely exposed in both Graham Land and the South Shetland Islands.

Unfolded sedimentary and volcanic rocks of Jurassic age overlie the Trinity Peninsula Series, and Miocene to Recent volcanic rocks occur at James Ross Island and in the South Shetland Islands (Adie, 1962). The Basement Complex is exposed in the south-west of Graham Land (Adie, 1962).

III. INSTRUMENTATION AND SURVEY TECHNIQUE

1. *Instrumentation*

Cox (1964) has described the instrumentation for marine seismic refraction survey used by the Department of Geology, University of Birmingham, in association with the British Antarctic Survey. The instrumentation for the present survey was improved by the purchase of a four-channel amplifier

and filter system (GTR 200) manufactured by Dresser Electronics, and an ultra-violet recorder manufactured by New Electronic Products Ltd. Timing lines were provided by a scaled-down 10 kc./sec. crystal oscillator. Two low output impedance crystal hydrophones were used to detect the seismic waves produced by the shots. The amplifier-filter system yielded two outputs with high and low band-pass filtering for each of the hydrophone inputs. Each of these outputs was also provided for recording at an attenuated level. This facility was incorporated so that detail in high-amplitude events was not lost. Unfortunately, the specified difference of 15 db. between the low- and high-level signals produced by the amplifiers was not realized, because the amplifiers were not properly matched to the galvanometers of the recorder. Eight channels were used for recording the hydrophone signals, whilst two were used for timing lines and one each for the shot instant and Asdic which were transmitted by radio from H.M.S. *Protector*.

The hydrophone flotation system was modelled on that used by Scripps Institute of Oceanography (Shor, 1963). A 200 m. length of cable, arranged for positive buoyancy, was streamed from the stern of R.R.S. *Shackleton*, which acted as the recording ship. A cable 50 m. in length was weighted at its lower end and suspended from the end of the streamed cable. Two cables with neutral buoyancy were attached to the bottom of the weighted cable and a hydrophone was attached to the end of each. The hydrophones themselves were given neutral buoyancy by mounting them in varnished wooden blocks. The flotation system was designed to position the hydrophones at a depth of about 50 m. below sea-level. The hydrophone cable was slackened shortly before the onset of the arrivals from the shot, so that the hydrophones were stationary in the water on reception of the seismic signals. Ship noise was reduced to a minimum by switching off non-essential plant.

2. *Technique*

Naval demolition charges ranging in size from 10 to 250 lb. (4·5 to 114 kg.) and 300 lb. (136 kg.) depth charges were fired from H.M.S. *Protector*. The charges up to 250 lb. (114 kg.) in weight were fired electrically, whilst the depth charges were fired by pressure fuses. The shot instant was determined from the instant of electrical detonation or from the ship's Asdic in the case of the depth charges. Tests of the delay between the firing of the detonators and the surge of the detonating current gave a satisfactory figure of about 0·01 sec. The shot instant or Asdic record was transmitted by radio to the receiving ship. The depth of water at each shot location was recorded and the positions of individual shots were calculated from radar, water-wave range and dead reckoning.

In the deep-sea areas of the Scotia Sea (lines D to J) shots were fired at 1 mile* (1·85 km.) intervals from the range at which refraction arrivals occurred as first events (generally about 5 miles (9·3 km.)) out to a range of about 10 miles (18·5 km.). A 2 mile (3·7 km.) shot spacing was used between 10 and 20 miles (18·5 and 37·0 km.) and a spacing of 3 miles (5·6 km.) was used out to maximum attainable range. This shot spacing was just adequate, if no misfiring of the charges occurred. However, the survey would have been more valuable if shots at approximately 0·5 mile (0·93 km.) spacing had been fired from the position of the receiving ship out to a range of about 5 miles (9·3 km.). A closer spacing of shots at these distances would have given information which would have been valuable for a more comprehensive study of the sea-bottom reflections than has been possible (p. 14).

The maximum length of seismic line shot in the deep-water areas of the Scotia Sea was 36 miles (66·7 km.) and the average length of line was 27 miles (50·0 km.). The average wind strength during the survey of the Scotia Sea was 14 kt. (7·2 m./sec.) with a maximum of 29 kt. (14·9 m./sec.) on line J_R. The sea swell averaged an estimated 5·5 ft. (1·7 m.) with a maximum of 8 ft. (2·4 m.) on line J_R.

The shooting technique allowed a given sinking time for each charge weight before detonation. This time was limited by the length of the firing cable and the effect of the shock wave from the charge on the shooting ship. Sinking times of 25, 30, 45 and 65 sec. were allowed for charge sizes of 50, 75–100, 200–250 and 300 lb. (22·7, 34–45, 91–114 and 136 kg.), respectively. On an average line of about 3 km. water depth these charges were adequate for ranges of 5–7, 8–12, 14–23 and 26 miles (9·3–13·0, 14·8–22·2, 25·9–42·6 and 48·2 km.), respectively. Charges above 25 lb. (11·4 kg.) weight sank at about 10 ft. (3·0 m.)/sec. (personal communication from W. Ashcroft) and the depth charges sank at $10{\cdot}5 \pm 1{\cdot}0$ ft. $(3{\cdot}2 \pm 0{\cdot}3$ m.)/sec.

* Throughout this report the "mile" unit refers to "nautical miles", i.e. 1 nautical mile = 1·852 km.

There is an optimum depth at which each charge size should be fired. This depth should be equal to the quarter wave-length, corresponding to the bubble-pulse period. If the shot is fired at this depth, then the wave which has been reflected at the sea surface will have the same phase on returning to the shot depth as the first bubble pulse, and constructive interference will reinforce the amplitude of the first bubble pulse as it travels down to the sea bed. The bubble-pulse frequency, f, for TNT is determined by the equation

$$f = \frac{(H+33)^{\frac{5}{6}}}{4{\cdot}36W^{\frac{1}{3}}}, \tag{1}$$

where the units of depth are in feet and the units of the charge weight, W, are in pounds (Shor, 1963). At the optimum quarter-wave depth, $H = v_0/4f$ and therefore

$$H(H+33)^{\frac{5}{6}} = 1{\cdot}09\ v_0 W^{\frac{1}{3}}, \tag{2}$$

where v_0 is the velocity of sound in sea-water. v_0 has a value of approximately 1·45 km./sec. in the shallow depths of the Scotia Sea. Fig. 2 indicates the optimum and actual depths for each charge. From this it is clear that the charges were not fired at the optimum depths, but it is hoped that in future investigations it might be possible to reduce the charge-sinking times.

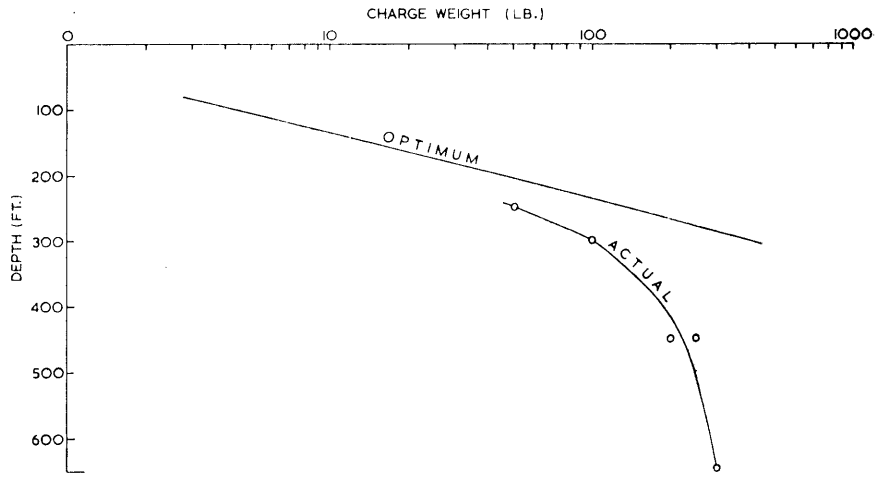

FIGURE 2
Optimum and actual charge depths.

3. *Criticisms of survey technique*

An analysis of the survey technique indicates it could be improved in the following ways:

i. Some of the materials used in the hydrophone flotation system were not waterproof, so that the buoyancy of the system changed during the time the hydrophones were in the water. This failing has been remedied for survey in subsequent years.

ii. The charges were not fired at the optimum depths. It is difficult to estimate how much improvement in signal strength would have been achieved by firing at the correct depths, but it is clear that the amplitude of the interference product of the surface reflection and the first bubble pulse may be twice that of the first bubble pulse, if the correct shooting depth is used.

iii. The average wind strength was 14 kt. (7·2 m./sec.) during the survey. This figure is probably greater than that generally encountered during most seismic surveys and it no doubt contributed to the maximum ranges of the seismic lines being somewhat smaller than those generally achieved for similar charge sizes and sea depths.

iv. The interpretation of the survey would have been more accurate, if more information on the shallow refractors on and beneath the sea bed had been obtained. The velocity and density of the sea-bed sediments could have been determined more accurately, if a series of closely spaced shots had been fired at short ranges from the receiving ship.

IV. DETERMINATION OF SEA-BED SEDIMENT CHARACTERISTICS FROM SEISMIC REFLECTION DATA

MARINE seismic refraction surveys are primarily undertaken to obtain information on the nature and thickness of crustal rocks beneath the sea bed. In areas where the depth of the sea is several kilometres, the velocities of the uppermost layers are often not determined by a conventional seismic refraction survey. The refraction arrivals from the uppermost sediment layers occur late on the seismogram and they are often obscured by the refractions from deeper layers which arrive earlier. Consequently, any information that can be obtained from reflections arriving after the direct wave on the records is most useful. If the seismograms are recorded so that the various reflections of the shot impulse between the sea bed and the sea surface are included together with other more complicated propagation modes, then the characteristics of these modes can be used to provide some information on shallow-sediment velocities.

The large charges used to produce a high signal to noise ratio in the refractions from the deeper layers of the Earth's crust are a liability in the study of reflection data. Seismic recording cameras, developed for conventional seismic refraction survey, often do not have the dynamic range to record all the detail of the large-amplitude reflection events produced by such changes. Moreover, paper speeds, which are adequate for the recording of the details of a 30 c./sec. refracted wave are often too slow for shot depth as the first bubble pulse, and constructive interference will reinforce the amplitude of the recording the detail of the higher frequency direct or reflected waves. The seismograms recorded during the present survey suffered from one or both of these defects, and it is only recently that the Department of Geology, University of Birmingham, has acquired the facilities for recording each hydrophone signal input at two levels. This system makes examination of reflection events much easier.

Many orders of reflected events were observed on the seismic records. These reflections are designated by an order which indicates the number of times they have been reflected at the sea floor. For instance, a second-order reflection event undergoes two reflections at the sea floor and one at the sea surface.

Reflection coefficients for the sea—sediment interface can be calculated by using an expression derived by Rayleigh (1945). The amplitude reflection coefficient, R, for plane waves reflected from a plane boundary between two fluids of densities, ρ_1 and ρ_2, and velocities, V_1 and V_2 is

$$R = \frac{\rho_2 \cos\theta - \rho_1(n^2 - \sin^2\theta)^{\frac{1}{2}}}{\rho_2 \cos\theta + \rho_1(n^2 - \sin^2\theta)^{\frac{1}{2}}}, \tag{3}$$

where $n = V_1/V_2$ is the index of refraction and θ is the angle of incidence of the plane wave at the fluid boundary. When the velocity of sound in the bottom sea-water is greater than that in the sediments of the sea bed, the reflection coefficient decreases from normal incidence and inverts at an angle given by

$$\theta_I = \cot^{-1}\left[\frac{1-n^{-2}}{(\rho_2 V_2/\rho_1 V_1)^2 - 1}\right]^{\frac{1}{2}}. \tag{4}$$

When the angle of incidence is greater than θ_I, the phase of the reflected wave is reversed by 180° with respect to the phase of the incident wave. The reflection coefficient increases rapidly to minus unity at an incident angle of 90°. When the sediment velocity is greater than the velocity of sound in the bottom sea-water, the reflection coefficient increases from that at normal incidence to unity at an angle of $\theta_c = \sin^{-1}(V_1/V_2)$. For angles of incidence greater than θ_c the reflected wave is changed in phase from 0° at θ_c to 180° at $\theta = 90°$.

The reflection coefficients determined from these formulae assume that the uppermost layers of the sea bed have no rigidity and can be considered as a liquid. Available evidence indicates that the rigidity of the sea-bed sediments is small (Fry and Raitt, 1961), so that these formulae are adequate for the investigation of sea-bottom reflections. The formulae also assume that the incident and reflected waves are planar and this will be the case for deep-sea seismic refraction survey. However, a further assumption that the sea bed is planar may restrict any analysis in areas of even gentle topography.

Katz and Ewing (1956), and Fry and Raitt (1961), have used the number of reflections recorded, with given survey geometry, and the range at which the reversal in phase of the first-order reflection occurs,

respectively, to obtain information on the sea-bed sediment velocity. Fry and Raitt studied the phase of the initial amplitudes of the first-order reflections on seismograms obtained over extensive areas of the Pacific Ocean. In many cases, where the sediment velocity was less than that of the bottom sea-water, it was shown that this amplitude decreases with increasing angle of incidence and eventually reverses in phase at angles between 74° and 80°. Having assumed a density for the sea-bed sediments, Fry and Raitt used the angle of incidence at which phase change occurs to obtain a measure of the velocity of sound in sediments of the sea floor. The method of Katz and Ewing can be used to determine the sea-bed sound velocity, when it is greater than the velocity of sound in the bottom sea-water. They assumed that the number of reflections on any seismic record is determined by the critical angle of incidence for the velocity configuration of the area under investigation. Dyk and Swainson (1953) have also noted the limited number of reflections for any one configuration of shot and receiver, and they again attributed this limit to reflection of the absent orders at angles less than the critical one. The limited number of reflections at any given range is best understood in terms of the variation of amplitude reflection coefficient with varying angles of incidence. Figs. 3a–c show the variation of the reflection coefficient for given

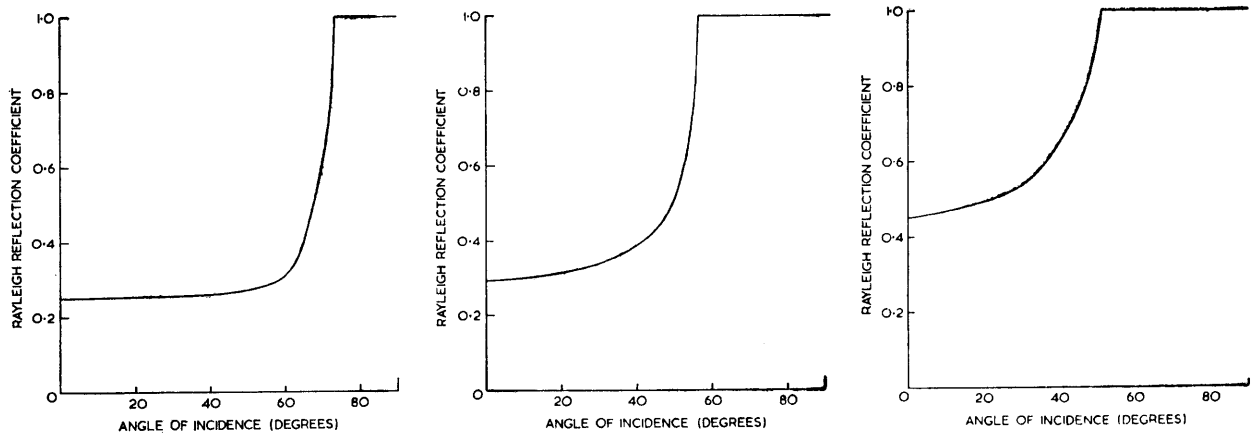

FIGURE 3

Variation in reflection coefficient for different angles of incidence.

a. Model 1; $v_1 = 1{\cdot}50$ km./sec., $\rho_1 = 1{\cdot}03$ g./cm.^{3}; $v_2 = 1{\cdot}58$ km./sec., $\rho_2 = 1{\cdot}60$ g./cm.^{3}.

b. Model 2; $v_1 = 1{\cdot}50$ km./sec., $\rho_1 = 1{\cdot}03$ g./cm.^{3}; $v_2 = 1{\cdot}80$ km./sec., $\rho_2 = 1{\cdot}60$ g./cm.^{3}.

c. Model 3; $v_1 = 1{\cdot}50$ km./sec., $\rho_1 = 1{\cdot}03$ g./cm.^{3}; $v_2 = 2{\cdot}10$ km./sec., $\rho_2 = 2{\cdot}0$ g./cm.^{3}.

ratios of sediment sound velocity and density to sea-water sound velocity and density. The limited number of reflections appearing on any given seismogram can be used to calculate the sediment sound velocity, when the velocity of sound in the sediments is greater than the velocity of sound in the bottom sea-water. The method of Fry and Raitt uses the phase change of the first-order reflection to determine sediment sound velocity when the sea-bed sediment velocity is less than the bottom sea-water velocity. When the sediment sound velocity is greater than that of the bottom sea-water, it can be seen from Figs. 3a–c that, for an angle of incidence below the critical angle for any multiple reflection, the amplitude reflection coefficient is less than unity and generally less than 0·5. When this reflection coefficient is raised to a power equal to the order of the multiple reflection, it can be seen that the overall amplitude of reflections will decrease rapidly with increasing order. Geometrical spreading of the seismic wave front also produces a decrease in the amplitude of the multiple reflections. This spreading loss will increase by 6 db. per doubling of reflection time, as the reflection amplitude decreases by a factor of two.

1. *Times of reflections*

A detailed study of reflections on lines D, D_R, E and E_R revealed reflections up to the sixth order. The time, R_n, of the nth order reflection is related to the direct-wave travel time, D, by the equation

$$R_n^2 = aD^2+b, \tag{5}$$

where a and b are constants. Plotting of the squared reflection and direct-wave travel times for line D_R

(Fig. 4) verified the linear relation implied by equation (5) and therefore confirmed the identification of the direct-wave and bottom-reflected arrivals. The times for reflection orders greater than four have not been plotted, because they are not seen on all records and because the higher order reflections have indistinct times of commencement. Multiple reflection times for the rest of the seismic lines were either plotted on similar graphs to Fig. 4 or calculated. No systematic deviations from the theoretical times were noted, although irregularities in the reflection times were often caused by variations in sea-bed topography. Hill (1952) noted systematic discrepancies between the theoretical and observed reflection

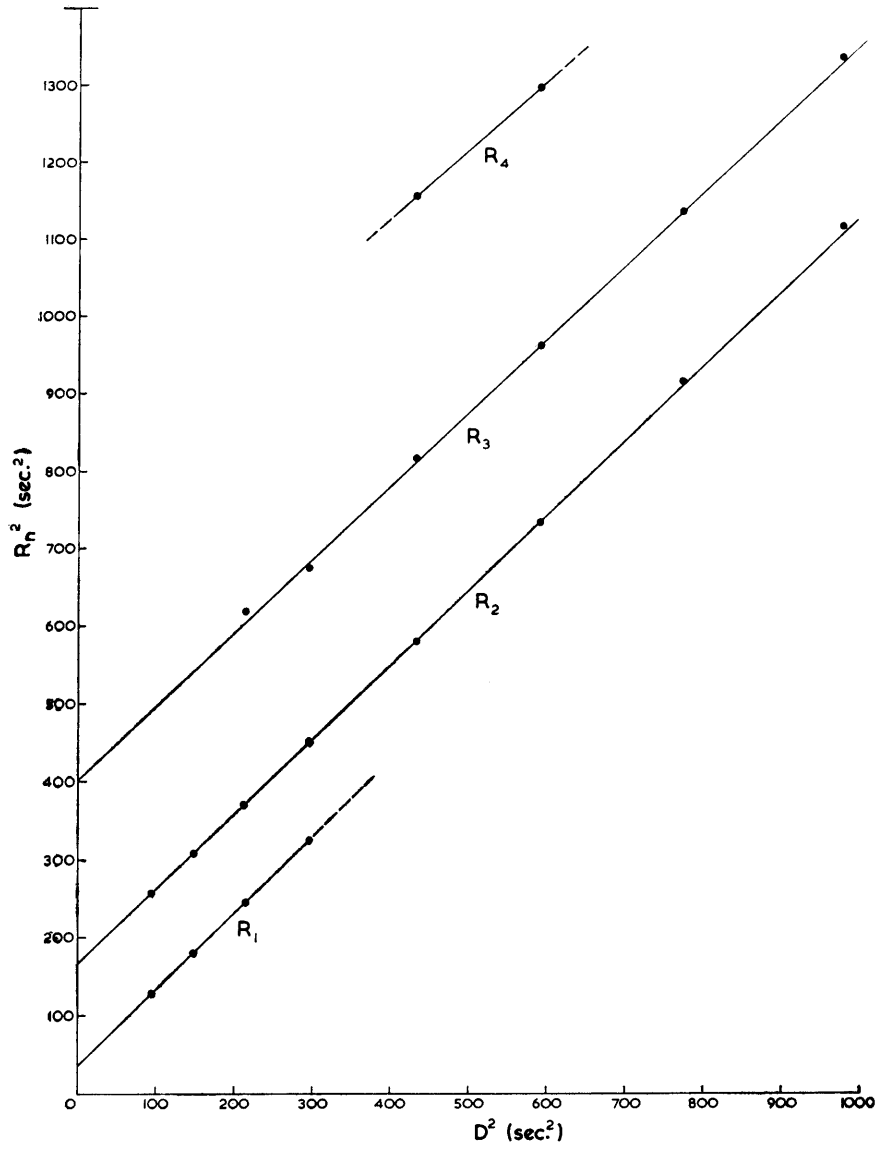

FIGURE 4
Reflection times for line E.

times during a survey in the Atlantic Ocean. These discrepancies became greater with increasing order of reflection and they led him to postulate that the seismic waves were penetrating the sea bed before being refracted back to the sea surface. He was able to calculate the velocity gradients in the sea-bed sediments which would produce the observed travel times. The lack of systematic discrepancies in the reflection times observed in the Scotia Sea indicates that there is little or no penetration of the sea-bed sediments. Katz and Ewing also found that the theoretical and observed reflection times were in agreement for their survey in the Atlantic Ocean.

2. *Sea-bed sediment sound velocities*

Lines D, D_R, E and E_R provided the clearest recording of multiple reflection events, and these lines were used to determine velocities of the uppermost sea-bed sediments by using the method of Katz and Ewing. Assuming that the number of reflections on a record is determined by the critical angle of reflection, that ray curvature is negligible and that the sea bed is horizontal, it can be shown that

$$v_m = v_v\left\{1+\frac{(2nH)^2}{v_0 D}\right\}^{\frac{1}{2}}, \tag{6}$$

where H is the water depth, n is the number of reflections, v_v is the mean vertical sound velocity, v_0 is the horizontal ranging velocity, v_m is the sound velocity beneath the reflector and D is the direct-wave travel time. This formula is easily proved by Pythagoras's Theorem but it does require that the direct wave is propagated with a velocity v_0 in the surface sound channel of the sea (p. 17).

The velocities of sound in the sea-bed sediments are given in Table I.

TABLE I

NUMBER OF REFLECTIONS AND SEA-BED SOUND VELOCITIES

Line Shot		*Number of Reflections Visible*	*Velocity* (km./sec.)	*Mean* (km./sec.)
D	68	3	2·50	
	72	5	2·10	
	73	5	2·41	
D_R	74	2	2·50	2·35
	77	3	2·25	
	80	5	2·32	
E	84	4	2·65	
	91	4	1·73	
E_R	97	4	2·13	2·10
	102	6	1·91	
	99	5	2·06	

It was sometimes difficult to decide the number of reflection orders present on the seismogram and the velocities given in Table I have been calculated from the certain minimum number of reflections on each record. A disadvantage of the determination of velocities using the method of Katz and Ewing can be the large horizontal range at which some of the reflections are observed. Clearly, it would be desirable to obtain a determination of sea-bed sediment velocity over a small horizontal range, so that the effects of variation in sea-bed topography can be minimized. It was therefore decided to investigate the variation in amplitude of the reflections from the sea floor in the hope that further information on the sea-bed sediment sound velocities might be obtained.

3. *Amplitudes of reflections*

The explosive charges fired during the course of the survey were generally made up from 10, 25 and 50 lb. (4·5, 11·4 and 22·7 kg.) units. Although all the explosive charges were primed, only

one or two of the units in a multiple charge were detonated electrically. The other units in the multiple charge were detonated sympathetically by their close proximity to the electrically detonated charges. This method of firing clearly could cause uncertainty in the amount of energy that is produced from given charge weights, and for this reason it was decided that a study of relative amplitudes of the first- and second-order reflections was preferable to a study of their absolute amplitudes. Since the clarity of reflections decreases with increasing order, a study of the ratios of the amplitudes of the first to second orders was considered most worthwhile, and the values of this ratio were computed for various angles of incidence. Straight ray paths were assumed to test the method at its simplest level. This assumption was later found to be adequate, because the quality of the data did not justify a more sophisticated curved-ray analysis. The angles of incidence for the first and second orders of reflection were calculated for various values of the ratio of range to depth, and the theoretical ratios of the first- to second-order reflection amplitudes were calculated from equation (11).

It can be shown (Wood, 1940) that the sound intensity of a plane progressive sinusoidal wave, I, is related to the root-mean-square pressure amplitude, p, and the characteristic acoustic impedance, Z, of the medium. Thus

$$I = p^2/Z. \tag{7}$$

This expression is a close approximation to the intensity of a seismic wave at large distances from the shot, where the wave front is approximately planar. The acoustic characteristic impedance is defined as the product of the density, ρ, and the velocity of sound in the medium, v, i.e. $Z = \rho v$. In large depths of water the assumption of spherical spreading of the seismic reflection wave front travelling towards the sea bed is applicable. If I_o is the seismic wave intensity at a short distance from the shot, then the intensity of sound at a great distance, r, is $I = I_o/4\pi r^2$, or in terms of the pressure amplitude, p,

$$\frac{p^2}{Z} = \frac{{p_o}^2}{4Z\pi r^2},$$

$$\text{or } p = \frac{p_o}{2r\pi^{\frac{1}{2}}}. \tag{8}$$

Analysis in terms of the pressure amplitudes is necessary, because the recording hydrophones are pressure-sensitive devices.

At large distances from the shot the seismic wave front which is propagating in the reflection mode towards the sea bed is approximately planar. Hence the use of Rayleigh reflection coefficients in the calculation of reflected-wave pressure amplitudes will introduce only small errors. If R_1 is the amplitude-reflection coefficient at the sea bed for the first-order reflection, then the strength of the image source below the sea bed is p_oR_1, and the pressure amplitude, p_1, recorded at the receiving hydrophone is

$$p_1 = \frac{p_oR_1}{2\pi^{\frac{1}{2}}(x^2+4z^2)^{\frac{1}{2}}}. \tag{9}$$

Similarly, if R_2 is the amplitude-reflection coefficient at the sea bed for the second-order reflection, then the strength of the image source below the sea bed (assuming a sea-surface reflection coefficient of unity) is $p_oR_2^2$ and the pressure amplitude recorded at the receiving hydrophone, p_2, is

$$p_2 = \frac{p_oR_2^2}{2\pi^{\frac{1}{2}}(x^2+16z^2)^{\frac{1}{2}}}. \tag{10}$$

Therefore, the ratio, Q, of the amplitudes of the first- and second-order reflections is

$$Q = \frac{p_1}{p_2} = \frac{R_1}{R_2^2} \cdot \frac{(x^2+16z^2)^{\frac{1}{2}}}{(x^2+4z^2)^{\frac{1}{2}}}$$

$$= \frac{R_1}{R_2^2} \cdot \frac{\{(x/z)^2+16\}^{\frac{1}{2}}}{\{(x/z)^2+4\}^{\frac{1}{2}}}. \tag{11}$$

It can be seen that the amplitude ratio is independent of charge size and receiver sensitivity, and that the spreading term is merely a function of the ratio of range to depth. It should be remembered, however,

that the propagation losses due to absorption and scattering have been neglected, although these losses are negligibly small for the frequencies and ranges under consideration (Horton, 1957).

The Rayleigh reflection coefficients were computed for three models of sea-water and sediment velocities and densities. All of these models used a sediment sound velocity greater than that of the bottom sea-water as a result of the sediment velocity determined by the Katz and Ewing method. The reflection coefficients for various angles of incidence are shown in Figs. 3a–c, where the subscripts "1" and "2" refer to the bottom sea-water and sediment, respectively.

If the ratios of the reflection amplitudes can be picked sufficiently accurately, then the construction of the best model to fit the observed data will yield information on the sea-bed sediment sound velocity and density. Lines E and E_R were examined and the amplitude ratios of the first- to the second-order reflections were obtained from the first motion amplitudes and from the envelopes of the reflections. The seismograms were by no means ideal for this investigation, since the dynamic range of the recording paper was sometimes too small for the charge size used and the paper speed was too slow to record the detail of the events clearly. Plate II shows the water wave and two reflections from the sea bottom obtained from shot 84. The amplitudes of the first motion of the first- and second-order reflections are difficult to measure on this seismogram, because of the closeness of the water-wave bubble pulse, W_3, to the first reflection and because of the background noise on the seismogram before the arrival of the second reflection. Nevertheless, it may be that future improvements in recording techniques and the directivity of the receiving hydrophone system may contribute to making these amplitude measurements more reliable.

The amplitude of the first reflection could not be measured beyond a given range of shot, because this reflection merges with the direct wave. (The difference in arrival time between the first-order reflection and the direct wave asymptotically approaches zero for a true reflection and a constant sea depth.) The first reflection often shows the repeated character of bubble pulses seen in the direct wave.

The observed amplitude ratios are shown in Fig. 5, and it can be seen that the theoretical ratio of the amplitudes of the first- and second-order reflections for model 2 of Fig. 3b provides the nearest fit to the observed data. Unfortunately, the ratio of the amplitudes of the first- and second-order reflections

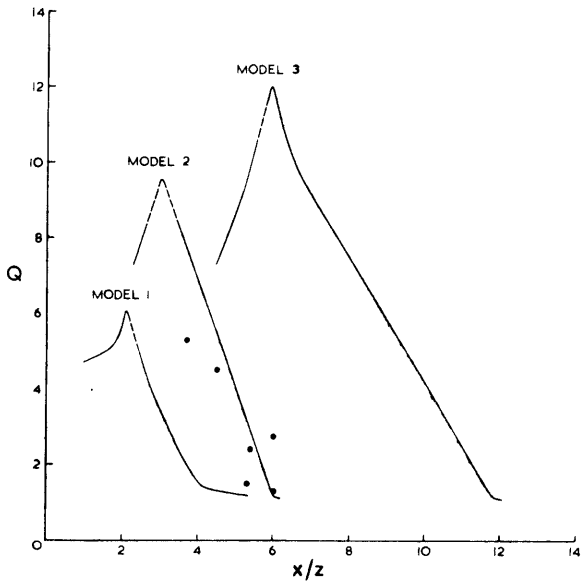

FIGURE 5

Variations in amplitude ratios for different ratios of shot range to water depth.
Model 1; $v_1 = 1{\cdot}50$ km./sec., $\rho_1 = 1{\cdot}03$ g./cm.^{3};
$v_2 = 1{\cdot}58$ km./sec., $\rho_2 = 1{\cdot}60$ g./cm.^{3}.
Model 2; $v_1 = 1{\cdot}50$ km./sec., $\rho_1 = 1{\cdot}03$ g./cm.^{3};
$v_2 = 1{\cdot}80$ km./sec., $\rho_2 = 1{\cdot}60$ g./cm.^{3}.
Model 3; $v_1 = 1{\cdot}50$ km./sec., $\rho_1 = 1{\cdot}03$ g./cm.^{3};
$v_2 = 2{\cdot}10$ km./sec., $\rho_2 = 2{\cdot}0$ g./cm.^{3}.

cannot be used with certainty to give an estimate of the sea-bed sediment velocity and density, if the velocity and density of model 2 (velocity equals 1·80 km./sec. and density equals 1·60 g./cm.^{3}) provide the best fit to the data. This restriction has been noted by Arons and Yennie (1950), who have observed the phase changes occurring on reflection for angles of incidence greater than critical when the sea-bed velocity is greater than the bottom sea-water velocity. They have emphasized that the reflection of the incident wave at high angles of incidence "so distorts its shape and amplitude that description in terms of [Rayleigh] reflection coefficients becomes virtually useless". With a velocity of 1·80 km./sec. and a density of 1·60 g./cm.^{3}, the critical angle for the first-order reflection is lower than the angles of incidence for all the first-order reflections recorded at their various ranges on lines E and E_R. Hence it may be that the amplitudes of the first-order reflections cannot be defined in terms of the Rayleigh reflection coefficient for the sediment characteristics under investigation.

If the method of Fry and Raitt is used to calculate the sea-bed reflection coefficient from the initial amplitudes of the first-order reflections, then it is found that the reflection coefficient calculated at long ranges falls significantly below the theoretical value of unity. In these calculations the reflection coefficient determined from the first-order reflection initial amplitude for shot 82 has been normalized at unity.

The approximate agreement between the reflection coefficients calculated for shots 82 and 83 (Table II) suggests that the Rayleigh reflection coefficients may be applicable at the ranges of these shots. The reflection coefficients calculated for shots 84 and 85 (Table II) suggest that the Rayleigh reflection coefficient cannot be used to calculate the amplitudes of sea-bottom reflections at longer ranges. Fry and Raitt have observed similar effects. It could be concluded that the amplitude ratios of the

TABLE II

CALCULATED REFLECTION COEFFICIENTS

Shot	*Calculated Reflection Coefficient*
82	1·0 (normalized)
83	1·1
84	0·5
85	0·7

first- and second-order reflections for shots 82 and 83 suggest that model 2 (sea-bed velocity of 1·80 km./sec. and density of 1·60 g./cm.^{3}) may be applicable to the sea-bed sediment characteristics. A sea-bed sediment velocity of 1·80 km./sec. provides some rough agreement with the velocity determined by the Katz and Ewing method, if the velocity determined from shot 84 is discarded as being inconsistently high. In this case, the Katz and Ewing method yields a velocity for the sea-bed sediments of 1·95 km./sec.

The calculations of the amplitude ratios for the first- and second-order reflections were made by using straight ray-path theory. The results of the study of amplitude ratios can best be described as semi-quantitative and correction for slight ray curvature is unwarranted. For investigations using data of higher quality, the application of curved-ray treatment will not fundamentally change the theory of the method.

4. *Criticism of the determination of sea-bed sediment sound velocity and density from a study of the amplitudes of reflections*

The determination of the sediment velocity and density, using the method of Fry and Raitt is simpler than the method devised for using the amplitude ratios of the first- and second-order reflections. Assuming that the seismic energy produced by an explosion is directly proportional to the charge size raised to the two-thirds power (Fry and Raitt, 1961, p. 594) and that the variations in receiver sensitivity are known, then the observed first-order reflection amplitudes need only be normalized to the value of the theoretical amplitude at zero angle of incidence and the shape of the curve fitted to the various models of sea-bed

sediment sound velocity and density. This method has the advantage that the amplitude of the second-order reflection, which may be difficult to measure, is not required. Provided that the amplitude of the shock wave produced by the explosive charge follows the law given by Fry and Raitt, then the method may be simpler and more accurate in use.

The determination of sediment velocities and densities from a study of the amplitude ratios of the first- and second-order reflections has an advantage over the method of Fry and Raitt in that no normalization is required. Hence, both the magnitudes of the curves and their shapes can be used in the investigation of the sea-bed sediment characteristics (Fig. 5). The amplitude ratio is also independent of charge size and receiver sensitivity, so that knowledge of the unknown efficiency of multiple charge detonation using electrical detonation of only one charge is not required. Although automatic gain control of the amplifiers was not used in this seismic survey, any such control would clearly require correction before the ratio between reflection amplitudes could be used.

It should be stressed that, since the method requires no normalization of the observed amplitude ratios, both the density and the velocity of sound propagation in the sediments are theoretically attainable. The quality of the results used to gain some approximate indication of sea-bottom sediment characteristics was not good enough to afford a stringent evaluation of the method but it is hoped that survey during future years will provide data for a closer examination.

5. R_{1b} *arrival*

The lack of certainty in the determination of sea-bed sediment velocity from sea-bottom reflection data makes examination of more complicated modes propagating by way of the sea bed worthwhile. If a sediment layer with a velocity greater than that of the sea bed occurs at a shallow depth below the sea bed, then seismic waves, which have a grazing angle of incidence at the sea bed, can be propagated as guided waves through the sea-bed sediment layer. This arrival, which has been designated R_{1b} by Katz and Ewing (1956), can be theoretically explained, if the velocity of the uppermost sediment layers is less than that of both the bottom sea-water and the underlying sediments. It should be noted that approximate determinations of the sea-bed sediment velocity indicates that this is greater than that of the bottom sea-water. The range at which the R_{1b} arrival will occur can be estimated from the range at which the RSR wave ray occurs. The RSR ray is the one grazing the sea bottom, which marks the maximum range at which the first-order reflection can be observed (Ewing, 1963). This range can be computed, if the velocity—depth structure of the sea is known. The most recent comprehensive information on the velocity of sound in sea-water in this area is still provided by the *Admiralty Tables* (Matthews, 1939). The velocity—depth structure given by Matthews can be approximately represented by a linear velocity increase with depth of the form $v = v_0 + ah$, where v is the velocity at a depth h, v_0 is the velocity at the sea surface and a is the velocity—depth gradient.

The seismic refraction survey from the South Orkney Islands to South Georgia extends over areas 28 and 29 of the *Admiralty Tables*, but the velocity distributions in these two areas are sufficiently similar to be treated as identical for the general conclusion drawn here. The variation of the interval velocity with depth of water can be calculated from the tables of average velocities listed by Matthews (1939), and a single velocity function can be obtained. v_0 was assumed as 1·454 km./sec. and a as 0·016 sec.$^{-1}$. The range at which grazing incidence at the sea bed occurs was calculated as 40·25 sec. for lines E and E_R from the formula (Nettleton, 1940, p. 259)

$$T = (2/a)\cosh^{-1}(v_m/v_0), \tag{12}$$

where T is the travel time of the direct wave in seconds, a is the velocity—depth gradient in sec.$^{-1}$, v_m is the velocity at the maximum sea depth and v_0 is the velocity at the sea surface. The proof of this formula is given by Nettleton (1940, p. 259). It becomes apparent from the above calculation that the range, at which the R_{1b} arrival could occur with the requisite water depth and velocity structure, is greater than the ranges reached on any line of the survey.

V. INTERPRETATION METHODS AND RESULTS OF THE SEISMIC REFRACTION SURVEY

A. Interpretation Methods

The interpretation of this survey is based on assumptions similar to those invoked by Drake, Ewing and Sutton (1959), who based their interpretation on four fundamental assumptions:

i. Each interface between two media or layers with different sound velocities is a plane and transmits refracted seismic energy at the velocity of sound in the lower layer. Deviations from this assumption are often observed when the interface is faulted or has topographic relief, but the assumption of a plane interface is usually invoked in the preliminary stages of the interpretation.

ii. A seismic wave with velocity V, travelling along an interface which has a dip of $\theta°$ with respect to the horizontal surface, will have an apparent velocity of $V/\cos\theta$ along the horizontal surface.

iii. Snell's Law is applicable to the refraction of a seismic wave propagating from one medium with velocity V_1 to a second medium with velocity V_2. If i_1 and i_2 are the angles of incidence with respect to the normal to the interface between the two media, then the following equation is valid:

$$\frac{\sin i_1}{\sin i_2} = \frac{V_1}{V_2}. \tag{13}$$

iv. The principle of reciprocity is applicable in that shot point and receiver can be interchanged without any change in travel time.

The travel times of the refracted waves are plotted against the times taken by the seismic waves to travel through the sea from the shot to the receiver. In land seismic refraction survey the refraction times are plotted against range but in marine survey the direct water-wave travel time is substituted for the ranging distance. If the assumptions listed above are applicable, then the plot of refraction times for one layer against direct-wave travel time will yield a graph with reciprocal slope proportional to the velocity of seismic wave propagation in the layer and an intercept on the ordinate axis which is proportional to the depth of the refractor below the surface. The graph is generally represented by the equation $t = x/V_1+t_1$, where t is the travel time for the refracted wave, x is the distance between shot and receiver, V_1 is the apparent velocity of the refractor at the surface and t_1 is the intercept time on the ordinate axis. When the distance between shot and receiver is measured in terms of the direct water-wave travel time (in seconds), then the reciprocal slope of the above graph must be multiplied by the velocity of propagation of the direct water wave to obtain the apparent velocity of the refractor.

If the refractors which are being mapped are not horizontal, then the apparent velocities of seismic wave propagation in these refractors will be greater for shots fired up-dip to the receiver and lower for shots fired down-dip to the receiver. It is therefore necessary to reverse the seismic line to find the true velocity and apparent dip along the line of the profile. If the apparent dip along the seismic refraction line is small, then the true velocity of the refractor is obtained to a close approximation by the average of the up- and down-dip velocities. Dobrin (1960) has given an exact analytical expression for the determination of the true velocity and apparent dip of the refractor along the length of the seismic refraction line. If θ is the slope of the refractor, V_D and V_U are the down-dip and up-dip apparent refractor velocities, V_o is the velocity of the layer whose top surface is horizontal and whose bottom surface has the dip of the underlying refractor which is being mapped, then the equation for the apparent dip of the refractor along the line is

$$\theta = \tfrac{1}{2}\,(\sin^{-1} V_o/V_D - \sin^{-1} V_o/V_U). \tag{14}$$

The true velocity, V_1, of the refractor is defined by

$$V_1 = \frac{2\cos\theta}{1/V_D+1/V_U}. \tag{15}$$

When θ is small, $\cos\theta$ approaches unity and the true velocity, V_1, approaches the mean of the up- and down-dip velocities. For the dips determined in the present survey the true velocity of the refractor is

equal to the mean of the apparent velocities, if this mean is given to only one decimal place. The dip, as determined by equation (14), is that of the refractor in the vertical plane through the seismic line. This dip may not be equal to the true dip and for this reason it is often called the apparent dip.

It should be noted that the fourth assumption listed above, namely, the principle involving the interchangeability of shot point and receiver, implies that the travel times for any one refractor should be the same for both lines at the same range. The travel-time graphs given in the results indicate that this assumption is often approximately applicable, although discrepancies can arise when the lines are not exactly reversed. The exact reversal of seismic lines at sea is often very difficult, because wind and currents can cause drifts of both the receiving and shooting ships which are difficult to estimate. For example, it would not be unusual for a ship to drift at a rate of 1 kt. in the Scotia Sea and, during the shooting of a seismic line with a length of about 30 miles (55·6 km.), the receiving ship might drift as much as 4 miles (7·4 km.).

The thicknesses of the refracting layers are calculated from the intercept times of the respective velocity lines on the travel-time graphs. The total intercept time can be generally expressed as

$$t_i = 2\sum_{k=1}^{n-1} \frac{h_k \cos i_k}{V_k}, \tag{16}$$

where V_k is the true velocity of the kth refractor, h_k is the thickness of the kth layer measured from the point at which the seismic ray path from the receiver enters the kth layer and perpendicular to the interface between the kth and the $(k+1)$th layers, and i_k is the angle made with the normal in the kth layer.

1. *Investigation of the water-wave propagation paths*

The ranges of the shots on the seismic lines are expressed in terms of the water-wave travel times on the travel-time graphs for each line. The slope of these graphs for each refractor requires multiplication by the appropriate water-wave propagation velocity for conversion to the apparent velocities of the refractors.

The seismic refraction survey extended over areas 28 and 29 of the *Admiralty Tables* (Matthews, 1939) but the velocity—depth functions in the two areas are sufficiently similar to be considered the same for the general conclusions to be drawn from this section. Matthews has listed the average velocities in the two areas down to various depths. An investigation of the propagation paths of the direct water wave is more easily considered in terms of interval velocities or the velocities of sound propagation at given depths. Interval velocities have been obtained from the average velocities listed in the tables and three velocity—depth functions have been derived as the closest approximations to the velocity—depth data within their respective depth limits. These functions are $v = 1{\cdot}445$ km./sec.$+0{\cdot}070h$, $v = 1{\cdot}451$ km./sec.$+0{\cdot}018h$ and $v = 1{\cdot}454$ km./sec.$+0{\cdot}016h$ for depths less than 300 m., 2,000 m. and 5,000 m., respectively, where v is the velocity at depth h in km./sec. and h is the depth in km.

The propagation velocity of the direct water wave will vary with range in areas where the velocity of sound propagation in water increases with depth of water. For computational convenience, one average propagation velocity has been used for the direct water wave, since the effects of propagation velocity are not geologically significant over the average length of seismic line attained during the survey.

The average propagation velocity of 1·451 km./sec. in water depths less than 300 m. was chosen for the computation of the velocities of the refractors. Although this velocity will be a little high for the computation of some of the results from the seismic lines in shallow water, more detailed examination of the velocity—depth function for depths less than 2,000 m. revealed that an average velocity of 1·458 km./sec. would have been more appropriate for the seismic lines in deeper water. This average velocity was obtained from an application of a formula of the type $x = \frac{2v_o}{a} \sinh(aT/2)$ (Dix, 1952, p. 248) where x is the horizontal range, v_o is the velocity at the sea surface, a is the velocity—depth gradient and T is the water-wave travel time. It is estimated that the use of the average velocity 1·451 km./sec.

will introduce errors into the results which are rarely greater than 0·5 per cent and always less than 1 per cent. The calculated velocities, thicknesses and depths of the refractors will be susceptible to both this geologically insignificant error and the systematic errors discussed on p. 19.

2. *Shallow refractor information*

The interpretation of seismic refraction surveys in deep-water areas is often made difficult by the lack of good quality information from the uppermost layers. In the Scotia Sea area the crustal rocks are often overlain by refractors with velocities of about 2·0 and 3–4 km./sec. The refracted waves travel more slowly in these uppermost layers and they arrive at the receiver after the refracted waves from the deeper crustal rocks. The arrivals which are later than the first ones at the receiver are often difficult to pick from the seismogram, because they may occur in the wave trains of the first arrivals. In particular, most of the information on the velocity of seismic wave propagation in sea-bed sediments is often of poor quality or even absent, so that other techniques are sometimes necessary to give an indication of the sea-bed sediment velocity. Details of the methods of using reflections from the sea bed (which occur later than the direct water wave) to give an estimate of the sea-bed sediment velocity and density are discussed on p. 8-14. It is sufficient to remark here that a velocity of about 2·0 km./sec. is indicated for the sea-bed sediments and that this figure is in agreement with the velocity determined by Ewing and Ewing (personal communication) in widespread areas of the Scotia Sea.

3. *Datum corrections*

It is often necessary to make a correction for the topography of the sea bottom, so that variations in sea depth do not affect the determination of the refractor velocities and depths. A velocity of 2·0 km./sec. has been used for the datum correction of all of the seismic lines which were shot in deep water. Lines A, C and B, which were completed on the shelf of the South Orkney Islands, sometimes gave a lower velocity for the sea-bed sediments. The topographic relief on this shelf often did not merit any datum correction beyond the reduction of the observed times to those which would have been observed with the shots and receiver on the sea bed. Topographic variations of more than 100 m. are generally corrected by most authors (Le Pichon and others, 1965). In the present survey topographic variations of more than 110 m. were corrected to a horizontal datum. It should be noted, however, that it is the depth of water below the receiver and the shots, rather than the actual sea depth, which is used in datum corrections. The depth of water below the charges will vary with the allowed sinking times, but datum corrections are usually applied as a matter of routine when the actual sea depth varies by more than about 100 m. along the seismic line. The routine of datum correction is one of successive approximation. Travel times are first reduced to the sea bottom, using the velocities of the refractors determined from uncorrected data, and then a reduction to a horizontal datum is carried out, using refractor velocities determined from times reduced to the sea bottom.

A good example of the need for a horizontal datum correction is provided by line E, where the water depth varies from 2,725 to 3,750 m. Reduction of the travel times to sea bottom gave *two* velocities, 4·16 and 6·34 km./sec., whereas correction to a horizontal datum gave one good determination of 6·34 km./sec. On the other hand, datum reduction of the sea bottom times recorded on line C, which has a sea-depth variation of 170 m. but an effective topographic variation of 60 m., did not yield any change in refractor velocities or intercept times.

4. *Interpretation of reversed lines*

The basic interpretation of seismic refraction data and the various corrections which have been described above require no more than objective application to achieve a given quality of interpretation. The interpretation of reversed lines is, however, less objective. Drake and others (1959) have commented that, if good second arrivals are evident and if the refractors are not rapidly changing in depth and thickness, then the consideration of two lines as reversed is justified. If rapid changes in the nature of the refractors are expected, then the calculation of true velocities and dips of the refractors may be inaccurate. The interpretation of two lines as reversed under these circumstances is sometimes known as "forcing". Lines B and B_R are examples of lines which have been reversed but which require independent interpretation.

The velocities and intercept times on either side of a reversed line can give a good indication of the consistency of that line. If the lines are consistent, then up-dip velocities should be associated with larger intercept times and down-dip velocities with smaller intercept times. The reciprocal times for each refractor should also give an indication of the consistency between the two lines. The consideration of two lines as reversed during interpretation has the advantage that the dips of the refractor, and hence the depths, can be calculated from both intercept times and apparent velocities. The discrepancy between the two determinations of depth for each refractor can therefore give an indication of the possible error in the calculated refractor depth.

5. *Errors of interpretation*

The velocities and intercept times associated with the arrivals from each refractor have been calculated using the least-square method. The standard deviations of these velocities and intercept times have been calculated for all the refractors. Many authors do not consider the calculation of statistical errors worthwhile when systematic errors, such as unseen velocity variations, may have far more importance. However, an estimate of the error associated with, for instance, a velocity determination can give some indication of the accuracy of event picking or the topographic relief of a refractor. Furthermore, the errors associated with the fitting of a straight line to the travel-time data can sometimes be useful in deciding the best fit from several possible solutions.

B. Results

The standard deviations of velocities and intercept times have to be quoted to two decimal places in order to be meaningful. Intercept times and velocities are similarly quoted for consistency. In common with standard practice, the final values for velocities are quoted to one decimal place, since higher accuracy is not significant geologically nor justifiable in view of the systematic errors of unseen velocity and topographic variations probably involved in the survey. The thicknesses and depths of the refractors are given to two decimal places, so that some of the smaller thicknesses are meaningful, but it should be remembered that these thicknesses and depths are subject to the same uncertainties as the velocities and therefore should be read to one decimal place.

Where they are necessary for discussion of the interpretation, shot numbers are given on the travel-time graphs. Reversed lines are designated by the subscript "R". Values of velocity and intercept time assumed for the interpretation of a particular seismic line, and derived from information on other seismic lines or other sources, are given in brackets. True velocities determined from the mean of apparent velocities are accurate to one decimal place for the dips of the layers determined in the survey.

The interpretation of each seismic line is discussed separately in the order of its geographical position, from south to north. The geological significance of the seismic interpretation is discussed on p. 36-42.

1. *Line A*

This line was shot from a receiving position at lat. 62°00′S., long. 44°00′W. in a northerly direction. The line was located on the southern edge of the South Orkney Islands shelf in water depths varying from 941 to 741 m. Weather conditions were poor and results were obtained only for the uppermost layers. Corrections to a datum of 941 m. below sea-level, using a velocity of 1·77 km./sec. for the sea-bed sediment, gave the following data (Fig. 6):

$V_1 = 1{\cdot}78 \pm 0{\cdot}02$ km./sec. $\quad t_1 = 0{\cdot}20 \pm 0{\cdot}30$ sec.
$V_2 = 2{\cdot}26 \pm 0{\cdot}02$ km./sec. $\quad t_2 = 0{\cdot}15 \pm 0{\cdot}30$ sec.
$V_3 = 3{\cdot}74 \pm 0{\cdot}07$ km./sec. $\quad t_3 = 1{\cdot}46 \pm 0{\cdot}30$ sec.

It is apparent that the velocities and intercept times V_1, t_1 and V_2, t_2 are mutually inconsistent. It is unlikely that a substantial thickness of material with a velocity lower than 1·78 km./sec. forms the sea bed. This inconsistency could be resolved most simply by a change in the slope of the sea bed, but Fig. 6 indicates that such a change does not occur. It must therefore be assumed that the arrivals from the 1·78 km./sec. velocity refractor have been picked late. This is feasible when arrivals are being picked from the noise generated from earlier arrivals. Therefore, it has been assumed that the intercept time for this refractor is zero.

Deterioration in weather conditions did not allow reversal of this line, so it has been assumed that the above velocities are true velocities and that the rock layers are horizontal. The thicknesses and depths calculated at the receiving station are given in Table III.

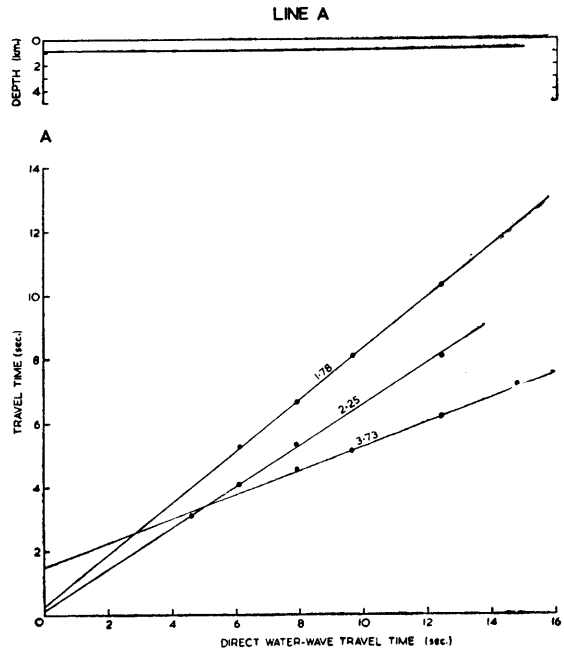

FIGURE 6
Travel times for line A.

TABLE III

RESULTS FOR LINE A

Velocity (km./sec.)	*Thickness* (km.)	*Depth* (km.)
1·45 (water)	0·94	0
1·8	0·22	0·94
2·3	1·75	1·16
3·7	Unknown	2·91

2. *Line C*

Line C was shot in a west-south-west direction from a receiving position at lat. 60°50'S., long. 44°14'W. Bad weather conditions again prevailed but slightly quieter hydrophone conditions were accomplished by positioning the ship in the lee of an iceberg. This line was shot on the South Orkney Islands shelf in water depths varying from 165 to 330 m. A datum correction to a depth of 265 m. below sea-level was applied, using a sea-bed velocity of 2·57 km./sec. which was determined on the adjacent line B. The following data were obtained (Fig. 7):

Shots 39–43 $V_2 = 3{\cdot}96 \pm 0{\cdot}20$ km./sec. $t_2 = 0{\cdot}07 \pm 0{\cdot}31$ sec.
Shots 34–41 $V_3 = 5{\cdot}66 \pm 0{\cdot}06$ km./sec. $t_3 = 0{\cdot}08 \pm 0{\cdot}08$ sec.
Shots 42–46 $V_3' = 5{\cdot}15 \pm 0{\cdot}01$ km./sec. $t_3' = -0{\cdot}01 \pm 0{\cdot}24$ sec.

Further data on the refractor with a velocity of 3·96 km./sec. was apparent at shorter ranges but the difficulty of separating these arrivals from probable multiply reflected refractions from the 5·66 km./sec.

velocity layer made these data unreliable. The mean depth of water in the area of the short-range shots was about 175 m., so that multiple reflections in the sea-water would have a delay of approximately 0·24 sec. It can be seen from Fig. 7 that some of the later arrivals have this order of time periodicity. The velocity of 5·15 km./sec. indicates a change in the apparent velocity from 5·66 km./sec. and there is no evidence to suggest whether this change is caused by a change in dip or true velocity. The thicknesses and depths of the refractors at the receiving station are given in Table IV.

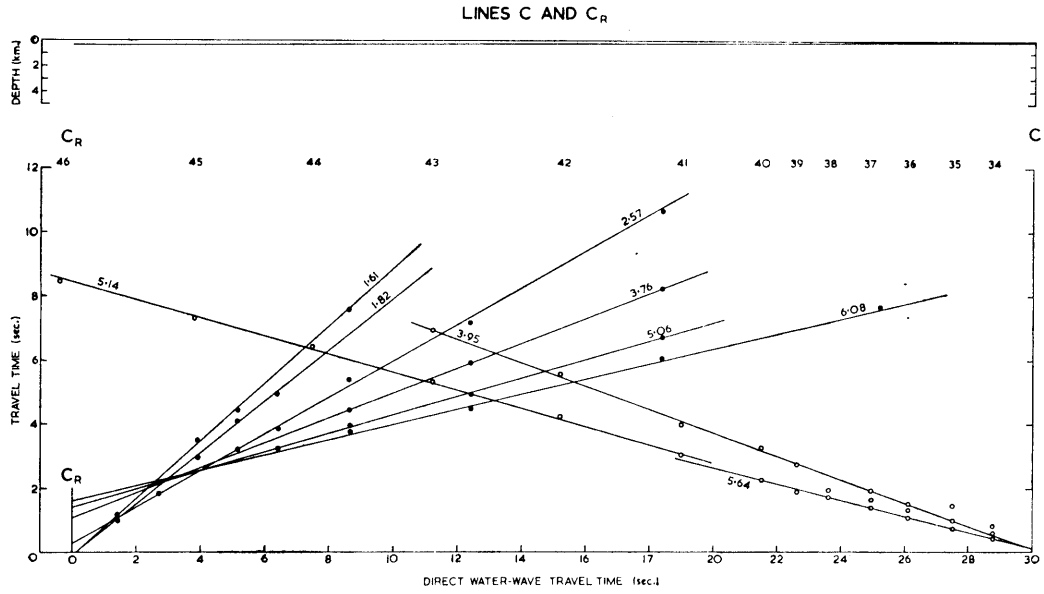

FIGURE 7
Travel times for lines C and C_R.

TABLE IV

RESULTS FOR LINE C

Velocity (km./sec.)	*Thickness* (km.)	*Depth* (km.)
1·45 (water)	0·17	0
(2·6)	0·21	0·17
4·0	0·03	0·38
5·7	Unknown	0·41

3. *Line* C_R

Variations in sea-bed topography of 110 m. made the correction of the travel times to the sea floor an adequate datum correction. This variation in the sea depth was slightly less than that recorded on line C, because that line was not exactly reversed. The receiving station for line C_R was positioned at lat. 61°10′S., long. 44°30′W., where the sea depth was 336 m. The following data were obtained (Fig. 7):

$V_1 = 1{\cdot}61 \pm 0{\cdot}06$ km./sec. $\quad t_1 = -0{\cdot}15 \pm 0{\cdot}30$ sec.
$V_2 = 1{\cdot}82 \pm 0{\cdot}02$ km./sec. $\quad t_2 = -0{\cdot}10 \pm 0{\cdot}10$ sec.
$V_3 = 2{\cdot}58 \pm 0{\cdot}05$ km./sec. $\quad t_3 = +0{\cdot}28 \pm 0{\cdot}24$ sec.
$V_4 = 3{\cdot}77 \pm 0{\cdot}02$ km./sec. $\quad t_4 = +1{\cdot}13 \pm 0{\cdot}08$ sec.
$V_5 = 5{\cdot}07 \pm 0{\cdot}04$ km./sec. $\quad t_5 = +1{\cdot}44 \pm 0{\cdot}14$ sec.
$V_6 = 6{\cdot}10 \pm 0{\cdot}02$ km./sec. $\quad t_6 = +1{\cdot}63 \pm 0{\cdot}12$ sec.

The negative intercept time, t_1, has no real geometrical interpretation if it is accepted that the velocity of 1·61 km./sec. is the velocity of the sea-bed sediments. The sea-bed topography is essentially smooth and would not be expected to produce such a negative intercept time. Both of the negative intercept times, t_1 and t_2, are most probably explained by early picking of late refraction arrivals of poor quality. It has been assumed that the intercept time, t_1, for the velocity of 1·61 km./sec. is zero and that the intercept time for V_2 is 0·05 sec.

Consideration of lines C and C_R as being reversed for the purpose of true-velocity and dip calculations is made difficult by the change in apparent velocity from 5·66 to 5·15 km./sec. on line C. The velocity of 5·15 km./sec. and its intercept time have been determined from arrivals at longer ranges on line C, and these are not consistent with a "down-dip" velocity corresponding to the 5·07 km./sec. velocity on line C. The information for the two lines has therefore been interpreted independently.

The thicknesses and depths of the refractors beneath the receiving station are given in Table V. The depths to the comparable refractors determined on line C are included for comparison in Table V.

TABLE V

RESULTS FOR LINE C_R

Velocity (km./sec.)	*Thickness* (km.)	*Depth* (km.)	*Depth on Line C* (km.)
1·45 (water)	0·34	0	0
1·6	0·09	0·34	—
1·8	0·26	0·43	—
2·6	0·38	0·69	0·17
3·8	0·39	2·07	0·38
5·1	0·50	2·46	0·41
6·1	Unknown	2·96	—

4. *Line B*

The receiving stations for lines B and C were virtually in the same position. Line B was shot in a north-north-east direction with the receiving ship again positioned in the lee of an iceberg to obtain quieter receiving conditions. The travel-time data were corrected to the sea bed, which was essentially horizontal at a depth of about 200 m., apart from a few shot positions at long ranges on the slope of the South Orkney Islands trench.

The following data were obtained (Fig. 8):

$V_1 = 2{\cdot}57 \pm 0{\cdot}07$ km./sec. $\quad t_1 = 0 \quad \pm 0{\cdot}50$ sec.
$V_2 = 4{\cdot}00 \pm 0{\cdot}14$ km./sec. $\quad t_2 = 0{\cdot}03 \pm 0{\cdot}42$ sec.
$V_3 = 5{\cdot}43 \pm 0{\cdot}19$ km./sec. $\quad t_3 = 0{\cdot}13 \pm 0{\cdot}27$ sec.

The velocity V_2 was modified to 3·73 km./sec. by the inclusion of arrivals at greater ranges but this velocity was not accepted, because of the difficulty of applying accurate corrections to the shots located in the trench. The accepted velocity for V_2 was determined from shots with essentially constant sea-depth positions. The velocity V_3 was unchanged by the inclusion of data from one shot located in deep water on the side of the trench.

In the discussion of line B_R it is shown that the lines B and B_R are best considered as single unreversed lines. Assuming horizontal layering, the thicknesses and depths of the refractors at the receiving station are given in Table VI.

A comparison of layer thicknesses at the receiving stations for lines B and C shows discrepancies. The discrepancy in the thickness of the 4·00 km./sec. layer on lines B and C is probably best explained by variations of the apparent velocity and dip of this refractor in the area.

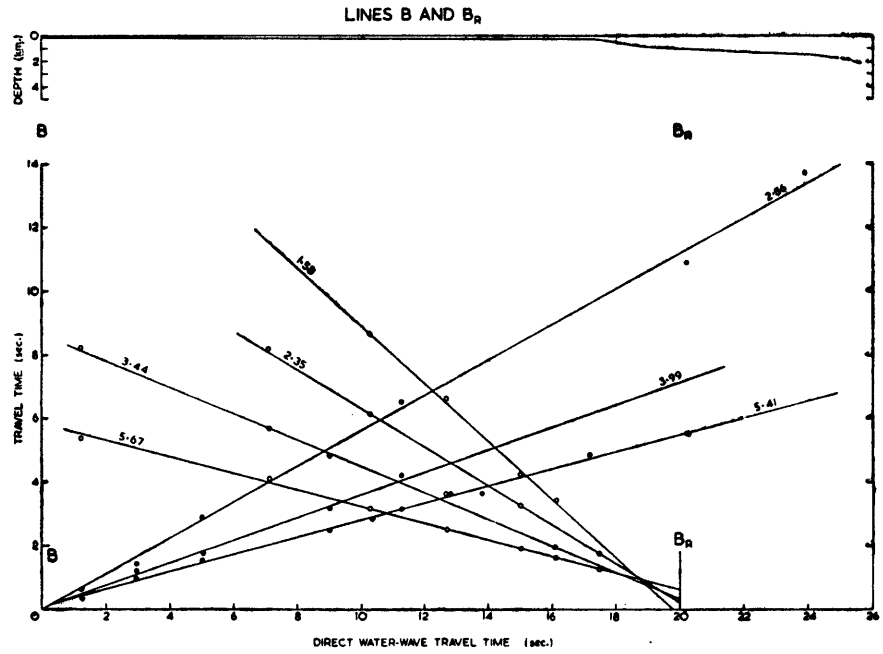

FIGURE 8

Travel times for lines B and B_R.

TABLE VI

RESULTS FOR LINE B

Velocity (km./sec.)	*Thickness* (km.)	*Depth* (km.)
1·45 (water)	0·16	0
2·6	0·05	0·16
4·0	0·38	0·21
5·4	Unknown	0·59

5. *Line B_R*

Line B_R was badly positioned, with the receiving station at lat. 60°32′S., long. 44°02′W. in a water depth of 1,100 m., whereas all the shots were fired in water depths varying from 100 to 200 m. Because of the slope of the sea bed in the area of the receiving station, a correction must be applied to the direct travel time of the water wave from each of the shots. The subtraction of delay times to reduce the observed travel times to those which would be observed on the sea bed is quite adequate, if the sea bed under the receiver is essentially horizontal. In this instance, however, a sea-bed slope of $\tan^{-1} 0{\cdot}245$ at the receiver must be taken into account. The effective receiver position must therefore be moved a distance of 230 m. to the south or, in other words, the travel time for the direct wave for each of the shots must be reduced by 0·16 sec. The following data (Fig. 8) were obtained after the application of the above corrections:

$V_1 = 1{\cdot}58 \pm 0{\cdot}06$ km./sec. $\quad t_1 = -0{\cdot}18 \pm 0{\cdot}40$ sec.
$V_2 = 2{\cdot}36 \pm 0{\cdot}09$ km./sec. $\quad t_2 = +0{\cdot}23 \pm 0{\cdot}36$ sec.
$V_3 = 3{\cdot}45 \pm 0{\cdot}07$ km./sec. $\quad t_3 = +0{\cdot}32 \pm 0{\cdot}27$ sec.
$V_4 = 5{\cdot}69 \pm 0{\cdot}07$ km./sec. $\quad t_4 = +0{\cdot}66 \pm 0{\cdot}20$ sec.

The negative intercept, t_1, is affected to some degree by the fact that all the shots which determine the velocity of the sea-bed refractor are in areas where the sea bed is horizontal and a good deal shallower

than the sea bed under the receiver. The path followed from the shots to the receiver shows a change in slope between the location of the shots and that of the receiver, which would make the intercept time for the velocity, V_1, less negative. It is difficult to give an exact estimate of this effect but it can only be expected to reduce the negative intercept time by about 0·03 sec. The rest of the negative intercept time is probably best explained by early picking of poor-quality late arrivals.

Lines B and B_R have been considered as single unreversed lines by assuming horizontal layering, because the velocities and intercept times on the two lines are inconsistent. The positioning of the receiving stations B and B_R in water depths which are largely different makes the reversed line treatment of little value when the layer thicknesses are small compared with the difference in water depths beneath receiving stations. The refractor thicknesses and depths at the receiving station are given in Table VII.

TABLE VII

RESULTS FOR LINE B_R

Velocity (km./sec.)	*Thickness* (km.)	*Depth* (km.)
1·45 (water)	1·10	0
1·6	0·25	1·10
2·4	0·07	1·35
3·5	0·65	1·42
5·7	Unknown	2·07

6. *Lines D and D_R*

Lines D and D_R were shot in an east—west direction along the South Orkney Islands trench from receiving stations at lat. 60°10′S., long. 43°28′W. and lat. 60°10′S., long. 44°22′W., respectively. The great depth of water, between 5,120 and 4,710 m., prevented refractions from the sea bed and the shallow refractor from appearing as first arrivals. The travel-time data for line D were reduced to a datum of 5,075 m. below sea-level and the following velocities and intercept times were determined (Fig. 9):

$V_3 = 6{\cdot}32 \pm 0{\cdot}04$ km./sec. $\quad t_3 = 1{\cdot}67 \pm 0{\cdot}49$ sec.

$V_4 = 8{\cdot}22 \pm 0{\cdot}04$ km./sec. $\quad t_4 = 2{\cdot}61 \pm 0{\cdot}15$ sec.

A velocity of 2·0 km./sec. was assumed to be the velocity of the uppermost sedimentary layer for the purpose of datum correction. Moreover, a velocity of 3·10 km./sec., which was determined on line E but undetected on lines D or D_R, was assumed to be present below the 2·0 km./sec. velocity layer on both lines D and D_R.

The travel-time data recorded on line D_R were reduced to a datum of 5,075 m. below sea-level. The following velocities and intercept times were determined (Fig. 9):

$V_3 = 5{\cdot}15 \pm 0{\cdot}05$ km./sec. $\quad t_3 = 0{\cdot}48 \pm 0{\cdot}21$ sec.

$V_4 = 6{\cdot}89 \pm 0{\cdot}12$ km./sec. $\quad t_4 = 1{\cdot}94 \pm 0{\cdot}57$ sec.

A comparison of the velocities and intercept times determined on lines D and D_R indicates that the two lines are sufficiently consistent to be interpreted as reversed lines. The mean or true velocities of the V_3 and V_4 refractors are thus determined as 5·7 and 7·6 km./sec. The depths and dips of these layers clearly depend on the assumed configuration of the refractors with velocities of 2·0 and 3·10 km./sec. It was assumed that the refractor with a velocity of 3·10 km./sec. was horizontal and occurred at a depth of 0·50 km. below the datum. A dip of 3°48′ from west to east was calculated for the refractor with true velocity of 5·7 km./sec. The discrepancy between the depth difference of the refractor at either end of the reversed profile, from calculations based on intercept times and apparent velocities, was a moderately satisfactory 0·4 km. This figure provides an estimate of the possible error in the determination of the depth of the refractor with the true velocity of 5·7 km./sec. The dip of the refractor with a velocity of 7·6 km./sec. is 0°22′ towards the west. The velocities and thicknesses of each layer are given in Table VIII, where assumed quantities are in brackets.

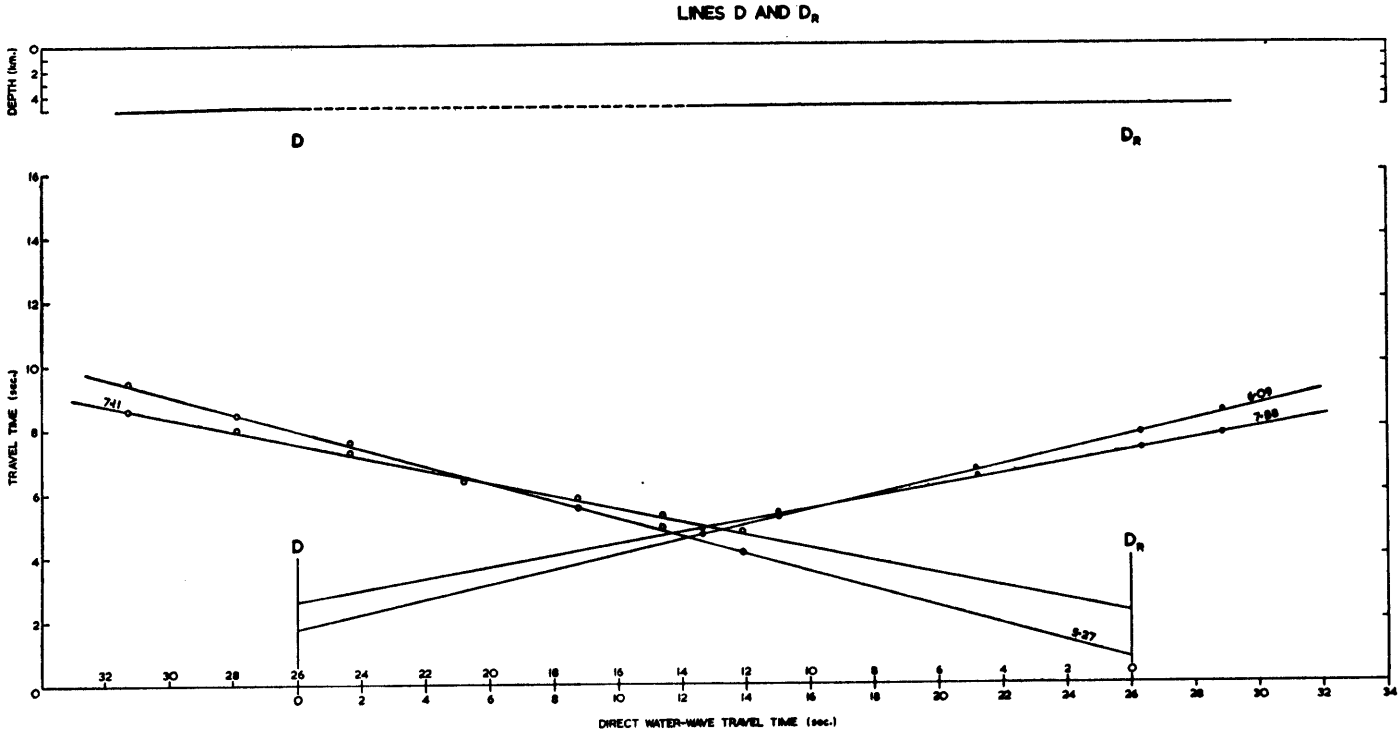

FIGURE 9
Travel times for lines D and D_R.

TABLE VIII

RESULTS FOR LINES D AND D_R

Line D		*Line D_R*	
Velocity (km./sec.)	*Thickness* (km.)	*Velocity* (km./sec.)	*Thickness* (km.)
1·47 (water)	4·96	1·47 (water)	4·71
(2·0)	0·61	(2·0)	0·86
(3·1)	0·04	(3·1)	2·28
6·3	3·44	5·2	6·35
8·2	Unknown	6·9	Unknown

TABLE IX

AVERAGED RESULTS FOR LINES D AND D_R

Velocity (km./sec.)	*Thickness* (km.)	*Depth to Refractor* (km.)
1·47 (water)	4·83	0
(2·0)	0·73	4·83
(3·1)	1·61	5·56
5·7	4·89	7·17
7·6	Unknown	12·06

The mean thicknesses and depths of the refractors are given in Table IX.

7. *Lines E and E_R*

These lines were shot in a north—south direction with the receiving station for line E at lat. 59°41′S., long. 44°09′W. and the receiving station for line E_R at lat. 59°18′S., long. 44°09′W. Water depths varied from 3,750 to 2,725 m. The travel times recorded on these two lines are mutually consistent enough for them to be considered as reversed. A sea-bed sediment velocity of 2·0 km./sec. was assumed and the data on both lines were corrected to 3,750 m. below sea-level. The following velocities and intercept times were obtained (Fig. 10):

Line E $V_3 = 6{\cdot}36 \pm 0{\cdot}07$ km./sec. $t_3 = 1{\cdot}49 \pm 0{\cdot}25$ sec.
Line E_R $V_2 = 3{\cdot}10 \pm 0{\cdot}05$ km./sec. $t_2 = 0{\cdot}38 \pm 0{\cdot}47$ sec.
$V_3 = 6{\cdot}08 \pm 0{\cdot}04$ km./sec. $t_3 = 1{\cdot}22 \pm 0{\cdot}20$ sec.

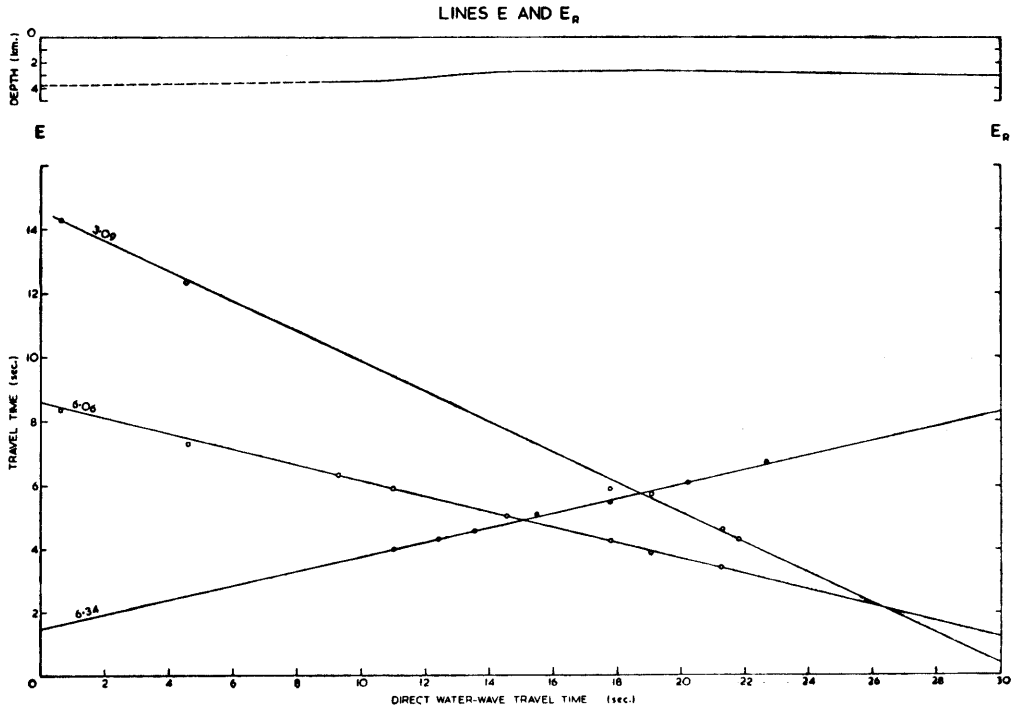

FIGURE 10

Travel times for lines E and E_R.

If the base of the 2·0 km./sec. velocity layer is assumed to be horizontal at a depth of 0·50 km. below the datum, then the dip of the refractor with the true velocity of 6·2 km./sec. is found to be 0°45′ in a southerly direction. The true velocities and thicknesses at the receiving stations are given in Table X,

TABLE X

RESULTS FOR LINES E AND E_R

Line E		*Line E_R*	
Velocity (km./sec.)	*Thickness* (km.)	*Velocity* (km./sec.)	*Thickness* (km.)
1·47 (water)	3·75	1·47 (water)	3·02
(2·0)	(0·50)	(2·0)	(1·23)
(3·1)	1·82	3·1	1·32
6·4	Unknown	6·1	Unknown

where the quantities in brackets are those that have been assumed. The discrepancy between the differences in refractor depth calculated between receiving points E and E_R, using intercept times and apparent velocities, is 0·08 km. This very small discrepancy is an indication that the assumptions used previous to the calculation of the layer thicknesses are at least approximately applicable. The mean thicknesses, velocities and depths of the layers are given in Table XI. The average thickness of the layer with a velocity

TABLE XI

AVERAGED RESULTS FOR LINES E AND E_R

Mean Velocity (km./sec.)	*Mean Thickness* (km.)	*Depth to Refractor* (km.)
1·47 (water)	3·38	0
(2·0)	0·86	3·38
3·1	1·57	4·24
6·2	Unknown	5·81

of 3·1 km./sec. is in good agreement with the average thickness of the layer assumed to be present on lines D and D_R.

8. *Lines F and F_R*

These two lines were shot in a north—south direction with the receiving station for line F at lat. 58°38′S., long. 43°54′W. and the receiving station for line F_R at lat. 58°07′S., long. 43°55′W. The water depth varied from 2,010 to 3,380 m. A sea-bed sediment velocity of 2·0 km./sec. was assumed and the data for both lines were corrected to a datum of 3,030 m. below sea-level. The following velocities and intercept times were obtained (Fig. 11):

Line F $V_2 = 2{\cdot}45 \pm 0{\cdot}03$ km./sec. $t_2 = 0 \quad \pm 0{\cdot}29$ sec.
$V_3 = 2{\cdot}86 \pm 0{\cdot}04$ km./sec. $t_3 = 0{\cdot}21 \pm 0{\cdot}42$ sec.
$V_4 = 5{\cdot}30 \pm 0{\cdot}01$ km./sec. $t_4 = 0{\cdot}65 \pm 0{\cdot}13$ sec.
$V_4' = 5{\cdot}53 \pm 0{\cdot}04$ km./sec. $t_4' = 0{\cdot}68 \pm 0{\cdot}38$ sec.
$V_5 = 4{\cdot}15 \pm 0{\cdot}04$ km./sec. $t_5 = 2{\cdot}23 \pm 0{\cdot}35$ sec.
Line F_R $V_4 = 6{\cdot}13 \pm 0{\cdot}04$ km./sec. $t_4 = 1{\cdot}42 \pm 0{\cdot}28$ sec.

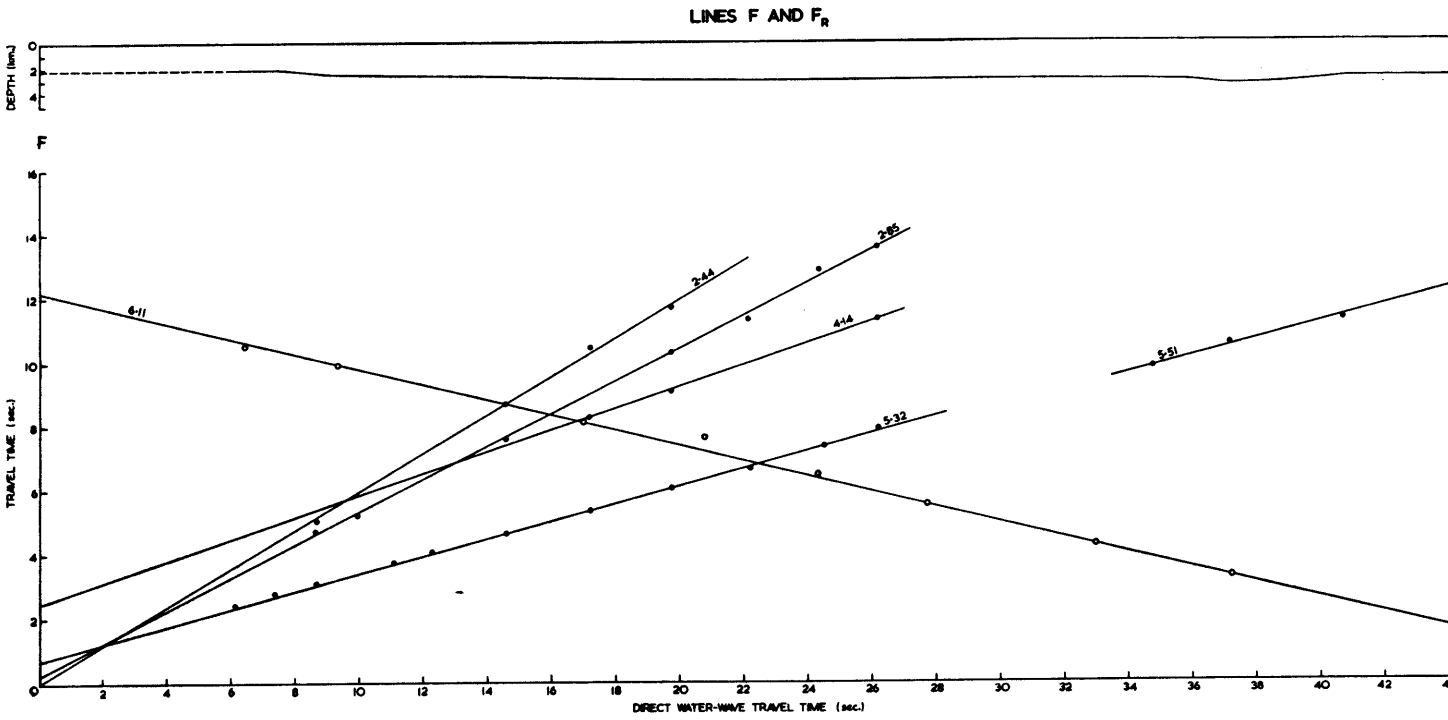

FIGURE 11
Travel times for lines F and F_R.

The interfaces between the layers with velocities V_1, V_2 and V_3 were assumed to be horizontal, because the refractions from these layers were recorded only on Line F. The V_4 refractor velocity changes from 5·30 to 5·53 km./sec. on line F. The velocity V_5 on line F could only be interpreted as shear velocity from a refractor deeper than the layer with an apparent velocity of 5·30 km./sec. A compressional-wave velocity of 7·35 km./sec. has been calculated from ratios between compressional- and shear-wave velocities obtained by Ewing, Ludwig and Ewing (1964) in the Argentine Basin. They obtained a mean ratio of 1·77 for refractors with compressional-wave velocities greater than 6·40 km./sec.

The thicknesses computed for the refractors on lines F and F_R are given in Table XII, where the quantities in brackets are assumed.

TABLE XII

RESULTS FOR LINES F AND F_R

Line F		*Line F_R*	
Velocity (km./sec.)	*Thickness* (km.)	*Velocity* (km./sec.)	*Thickness* (km.)
1·47 (water)	2·13	1·47 (water)	2·80
(2·0)	0·90	(2·0)	0·23
2·5	0·50	(2·5)	0·50
2·9	0·46	(2·9)	1·73
5·3	7·02	6·1	5·75
7·4	Unknown	(7·4)	Unknown

A dip of 2°30′ was calculated for the refractor with the true velocity of 5·7 km./sec., and a discrepancy of 1·4 km. was obtained for the difference in depth of this refractor between the receiving positions F and F_R calculated from intercept times and apparent velocities. This discrepancy provides an estimate of the possible error in the depth determinations for the two deeper refractors. The mean thicknesses and velocities of the layers and their depths below the sea surface are given in Table XIII.

TABLE XIII

AVERAGED RESULTS FOR LINES F AND F_R

Velocity (km./sec.)	*Thickness* (km.)	*Depth* (km.)
1·47 (water)	2·46	0
(2·0)	0·56	2·46
2·5	(0·50)	3·02
2·9	1·10	3·52
5·7	6·38	4·62
7·4	Unknown	11·00

9. *Lines G and G_R*

These two lines were shot in a north—south direction with the receiving station for line G at lat. 57°29′S., long. 43°41′W., and the receiving station for line G_R at lat. 57°08′S., long. 43°42′W. The water depth varied from 2,470 to 2,835 m. A sea-bed sediment velocity of 2·0 km./sec. was assumed and the data on both lines were corrected to a datum of 2,835 m. below sea-level. The following velocities and intercept times were obtained (Fig. 12):

Line G $V_4 = 5{\cdot}76 \pm 0{\cdot}08$ km./sec. $t_4 = 1{\cdot}04 \pm 0{\cdot}29$ sec.
Line G_R $V_4 = 5{\cdot}54 \pm 0{\cdot}05$ km./sec. $t_4 = 1{\cdot}18 \pm 0{\cdot}18$ sec.

Arrivals from shallower refractors were not recorded. It was assumed that the velocity layers 2·5 and 2·9 km./sec. determined on line F were also present in the area of lines G and G_R. The velocities and intercept times for lines G and G_R show some inconsistency but the two lines have been considered as reversed, so that some estimate of the possible error in depth determination could be gained.

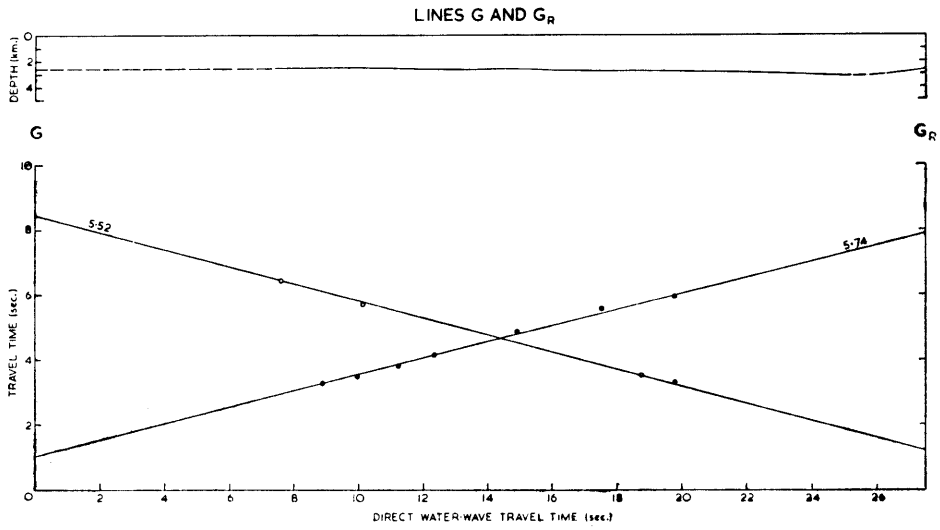

FIGURE 12

Travel times for lines G and G_R.

The base of the 2·0 km./sec. velocity layer was assumed to lie at a depth of 3,030 m. below sea-level as in lines F and F_R, and the thickness of 0·5 km. for the 2·5 km./sec. velocity layer determined on line F was assumed for lines G and G_R. The velocities and thicknesses of the refractor are given in Table XIV, where quantities in brackets are assumed.

TABLE XIV

RESULTS FOR LINES G AND G_R

Line G		*Line G_R*	
Velocity (km./sec.)	*Thickness* (km.)	*Velocity* (km./sec.)	*Thickness* (km.)
1·47 (water)	2·65	1·47 (water)	2·74
(2·0)	(0·38)	(2·0)	(0·29)
(2·5)	(0·50)	(2·5)	(0·50)
(2·9)	0·79	(2·9)	1·02
5·8	Unknown	5·5	Unknown

The mean velocities, thicknesses and depths of the refractors are given in Table XV. A dip of 0°40′ in a southerly direction was calculated from apparent velocities for the layer with a true velocity of 5·7 km./sec. However, the intercept times at the receiving stations G and G_R indicate a shallow dip in the opposite direction. The discrepancy between the differences in depths of this refractor at the receiving stations G and G_R, calculated from intercept times and apparent velocities, is 0·70 km. This discrepancy indicates the magnitude of possible error in the determination of depth to the deepest refractor.

TABLE XV

AVERAGED RESULTS FOR LINES G AND G_R

Velocity (km./sec.)	*Thickness* (km.)	*Depth to Refractor* (km.)
1·47 (water)	2·70	0
(2·0)	(0·33)	2·70
(2·5)	(0·50)	3·03
(2·9)	0·90	3·53
5·7	Unknown	4·43

10. *Lines H and H_R*

These two lines were shot in a north-east to south-west direction with the receiving position for line H at lat. 56°21′S., long. 43°26′W., and the receiving position for line H_R at lat. 56°00′S., long. 43°51′W. Water depths varied from 2,670 to 3,200 m. A sea-bed sediment velocity of 2·0 km/sec. was again assumed and the travel-time data on both lines were corrected to a datum of 3,200 m. below sea-level. The following velocities and intercept times (Fig. 13) were determined on the two lines after datum reduction:

Line H $V_3 = 5{\cdot}51 \pm 0{\cdot}02$ km./sec. $t_3 = 0{\cdot}37 \pm 0{\cdot}07$ sec.
Line H_R $V_3 = 6{\cdot}52 \pm 0{\cdot}03$ km./sec. $t_3 = 1{\cdot}48 \pm 0{\cdot}09$ sec.
$V_3' = 6{\cdot}57 \pm 0{\cdot}09$ km./sec. $t_3' = 1{\cdot}38 \pm 0{\cdot}53$ sec.

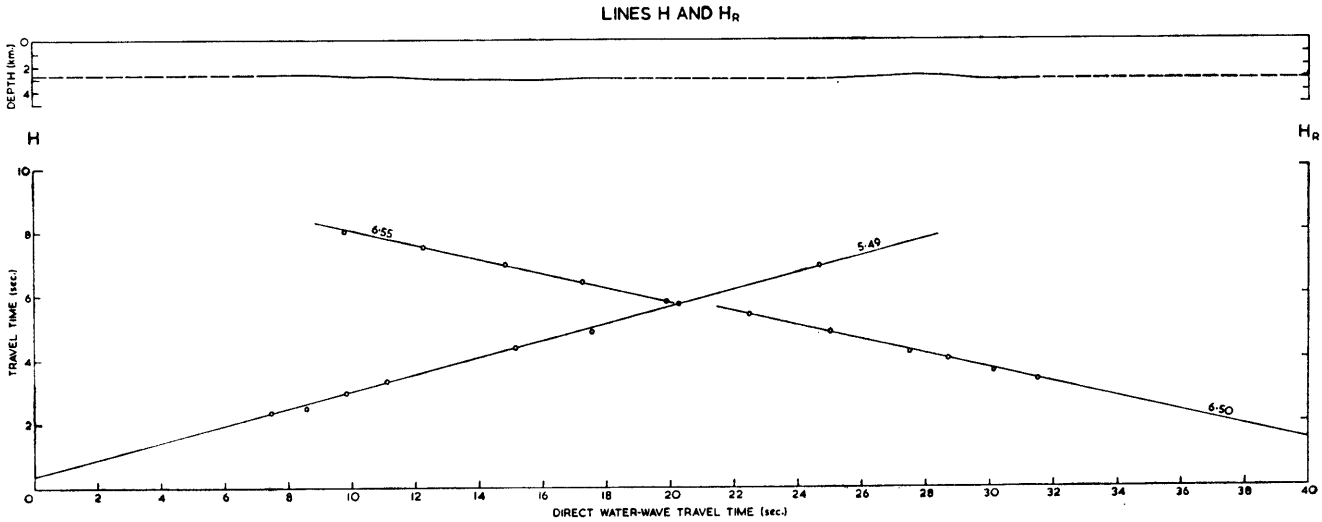

FIGURE 13

Travel times for lines H and H_R.

There is a discontinuity between the arrival times for V_3 and those for V_3' on line H_R (Fig. 13). This discontinuity was of approximately 0·20 sec. and it has been interpreted as a change in topography or a fault with a downthrow to the north.

Before layer thicknesses can be determined it is necessary to assume a velocity for the layer which probably occurs between the sea-bottom sediment and the V_3 refractor. Ewing and Ewing (personal communication) have determined a widespread velocity of 3·1 km./sec. in the Scotia Sea, and it has been assumed that a refractor with this velocity occurs in the vicinity of lines H and H_R. In the present survey an average velocity of 3·2 km./sec. for the second layer in deep-sea areas adds weight to the above assumption.

Lines H and H_R are consistent enough to be considered as reversed lines, and a true velocity of 6·0 km./sec. has been obtained for the V_3 refractor. The dip of this refractor is 1°50′ to the north. The layer with the assumed velocity of 3·1 km./sec. was assumed to be 0·50 km. thick, and the thickness of the other layers at the receiving stations are given in Table XVI, with assumed quantities in brackets.

TABLE XVI

RESULTS FOR LINES H AND H_R

Line H		*Line H_R*	
Velocity (km./sec.)	*Thickness* (km.)	*Velocity* (km./sec.)	*Thickness* (km.)
1·47 (water)	2·82	1·47 (water)	3·20
(2·0)	0·42	(2·0)	1·17
(3·1)	(0·50)	(3·1)	(0·50)
5·5	Unknown	6·5	Unknown

It should be noted that lines H and H_R have been considered as reversed, although there is no manifestation of a discontinuity on line H corresponding to the one on line H_R. These two lines are not exactly reversed so that it must be presumed that the topographic change has died out between the two lines. The topographic change observed on line H_R would have a magnitude of 0·40 km. if, as has been assumed, the thickness of the refractor with velocity 3·1 km./sec. is constant over the line H_R.

The discrepancy between intercept time and apparent velocity calculations for the difference in depth of the 6·0 km./sec. refractor at either end of the reversed line is 1·0 km. This gives an indication of the possible error which might be expected in the depth of the 6·0 km./sec. refractor.

The mean velocities, thicknesses and depths of the refractor are given in Table XVII, with assumed quantities in brackets.

TABLE XVII

AVERAGED RESULTS FOR LINES H AND H_R

Velocity (km./sec.)	*Thickness* (km.)	*Depth* (km.)
1·47 (water)	3·01	0
(2·0)	0·87	3·01
(3·1)	(0·50)	3·88
6·0	Unknown	4·38

If the discontinuity observed on line H_R is discounted, and one velocity and intercept time is determined from all the data, then the following is obtained:

$$V_3 = 6{\cdot}79 \text{ km./sec.} \qquad t_3 = 1{\cdot}58 \text{ sec.}$$

These data would modify the upper crustal true velocity of 6·0 km./sec., already determined, to 6·2 km./sec. Although there is good evidence on the travel-time plot that the discontinuity is real, no significant change in crustal velocity is obtained if it is neglected.

11. *Lines I and I_R*

Lines I and I_R were shot in a north-east to south-west direction with the receiving station for line I at lat. 55°27′S., long. 41°47′W., and the receiving station for line I_R at lat. 55°10′S., long. 41°13′W. Water depths varied from 3,070 to 3,630 m. Velocities of 2·0 and 3·6 km./sec. were determined on line J_R and these were assumed to be present on lines I and I_R. The data on both lines were corrected, using a sea-bed sediment velocity of 2·0 km./sec., to a datum of 3,630 m. below sea-level. Small time discontinuities were noted for the shallow refractor arrivals on both lines, and these could be assumed to be tentative indications of topographic changes or faulting of the refractor. Possible solutions for the data are discussed below.

If the small time discontinuities are ignored, then the following intercept times and apparent velocities are obtained:

Line I $V_3 = 5{\cdot}23 \pm 0{\cdot}10$ km./sec. $\quad t_3 = 0{\cdot}76 \pm 0{\cdot}34$ sec.
$V_4 = 7{\cdot}65 \pm 0{\cdot}05$ km./sec. $\quad t_4 = 2{\cdot}03 \pm 0{\cdot}24$ sec.
Line I_R $V_3 = 5{\cdot}47 \pm 0{\cdot}10$ km./sec. $\quad t_3 = 0{\cdot}65 \pm 0{\cdot}43$ sec.
$V_4 = 8{\cdot}27 \pm 0{\cdot}12$ km./sec. $\quad t_4 = 2{\cdot}31 \pm 0{\cdot}58$ sec.

The standard deviations of the velocity, V_3, on both lines are greater than those for most of the other lines in the survey, whilst the intercept times and the apparent velocities are inconsistent. Moreover, there is a large discrepancy in depths of the refractor, V_4, at the receiving stations I and I_R after calculation from intercept times and apparent velocities. This discrepancy amounts to the relatively large figure of 2 km. The interpretation is clearly weak enough to warrant a different interpretation of the travel-time data.

The discontinuities in the travel times from the refractor V_3 are recorded on both lines I and I_R, and possibly once in the arrivals from V_4 on line I_R. Generally, the discontinuities in the refracted arrivals from the layer V_3 are shown by offsetting of two arrivals from two shots on both lines I and I_R (Fig. 14). On line I_R, either the pair of arrivals from shots 193 and 194 or the pair of arrivals from shots 195 and 196 could be considered offset. In this case the arrivals are considered to be most consistently interpreted

when the offset pair gives a similar velocity to that given by the remainder of the arrivals. The following intercept times and apparent velocities have been obtained from different combinations of all the data:

Line I	Shots 182, 183, 184, 187	$V_3 = 6{\cdot}00 \pm 0{\cdot}02$ km./sec.	$t_3 = 1{\cdot}12 \pm 0{\cdot}08$ sec.
	Shots 185, 186	$V_3 = 5{\cdot}95$ km./sec.	
	Shots 189 to 192	$V_4 = 7{\cdot}39$ km./sec.	$t_4 = 1{\cdot}82$ sec.
	Shots 187 to 192	$V_4 = 7{\cdot}67$ km./sec.	$t_4 = 2{\cdot}04$ sec.
	Shots 187 to 192 (excluding 189)	$V_4 = 7{\cdot}76$ km./sec.	$t_4 = 2{\cdot}12$ sec.
	Shots 190 to 192	$V_4 = 7{\cdot}65$ km./sec.	$t_4 = 2{\cdot}04$ sec.
Line I_R	Shots 193, 194, 197, 198	$V_3 = 6{\cdot}42 \pm 0{\cdot}03$ km./sec.	$t_3 = 1{\cdot}38 \pm 0{\cdot}08$ sec.
	Shots 195, 196	$V_3 = 6{\cdot}17$ km./sec.	
	Shots 199 to 202 (excluding 200)	$V_4 = 8{\cdot}24$ km./sec.	$t_4 = 2{\cdot}58$ sec.
	Shots 199 to 202	$V_4 = 8{\cdot}27 \pm 0{\cdot}12$ km./sec.	$t_4 = 2{\cdot}42 \pm 0{\cdot}58$ sec.

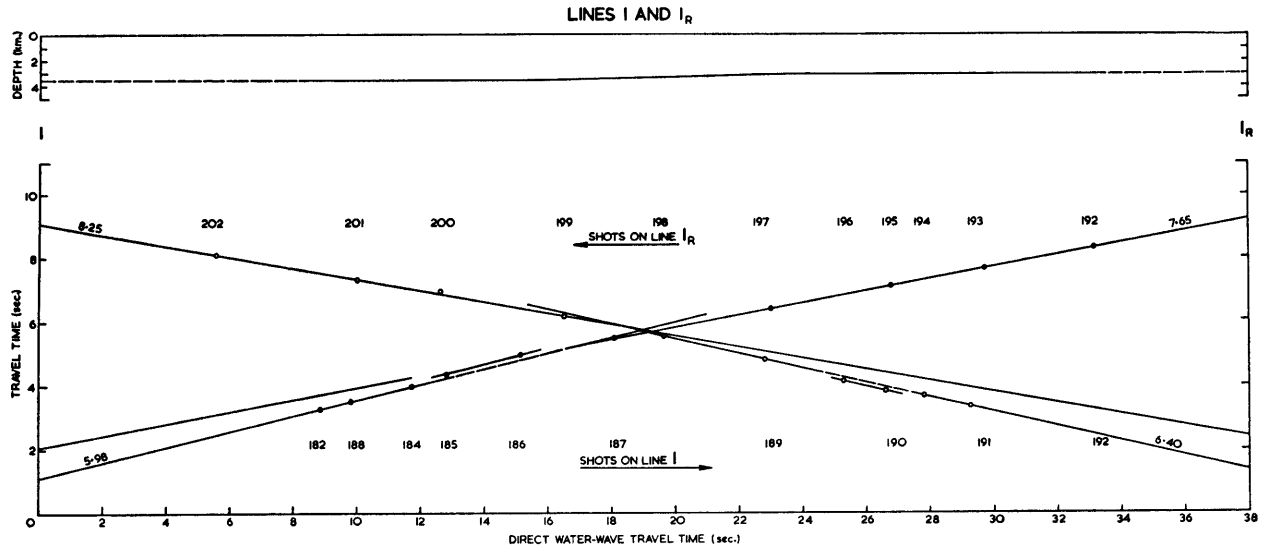

FIGURE 14

Travel times for lines I and I_R.

The solution for the refractions from layer V_3 is rated as satisfactory, because of the consistency of the apparent velocities and intercept times on each of the lines. It is difficult to correct the V_4 refraction times for the effect of the topographic variations observed on the refractor V_3, because the two lines I and I_R are not co-linear. Fortunately, the slight irregular variations in the refraction times for layer V_4 on both lines I and I_R have little effect on the determination of the V_4 velocity. Thus the apparent velocity of the V_4 refractor is 7·65 km./sec. for the good line given by shots 190–192 and 7·67 km./sec. for shots 187–192. The exclusion of shot 200 on line I_R also makes little difference to the determination of the V_4 apparent velocity. The following data were selected (Fig. 14):

Line I	$V_3 = 6{\cdot}00 \pm 0{\cdot}02$ km./sec.	$t_3 = 1{\cdot}12 \pm 0{\cdot}08$ sec.
	$V_4 = 7{\cdot}67 \pm 0{\cdot}05$ km./sec.	$t_4 = 2{\cdot}04 \pm 0{\cdot}25$ sec.
Line I_R	$V_3 = 6{\cdot}42 \pm 0{\cdot}03$ km./sec.	$t_3 = 1{\cdot}38 \pm 0{\cdot}08$ sec.
	$V_4 = 8{\cdot}27 \pm 0{\cdot}12$ km./sec.	$t_4 = 2{\cdot}42 \pm 0{\cdot}58$ sec.

The determination of the V_4 velocity on line I_R has a high standard deviation. This might be accounted for by the topographic changes which are responsible for the time discontinuities observed on the refraction arrivals from V_3. If the value of 8·24 km./sec. were selected for the V_4 velocity on line I_R, the intercept time would be increased by 0·16 sec. The choice of the final data (given above) implies that a deepening in the refractor V_3 occurs between shots 184 and 185 on line I, and that a shallowing of the same refractor occurs between shots 195 and 196 on line I_R. Alternatively, these variations in refractor topography might be explained by changes in the velocity of the layer overlying the V_3 refractor. The topographic changes will have a magnitude of about 0·4 km. and they could be represented by a graben feature on line I and a horst on line I_R. The dip of the refractor with the true velocity of 6·2 km./sec. is 0°40′ to the north. The discrepancy in the difference between the depth of the refractor under the receiving

stations I and I_R, using both intercept time and apparent velocity calculations, is 0·45 km. The dip of the refractor with the true velocity of 8·0 km./sec. is 0°10′ to the north, or the refractor is essentially horizontal. The velocities and thicknesses of the refractors at the receiving stations are given in Table XVIII, where quantities in brackets are assumed.

TABLE XVIII

RESULTS FOR LINES I AND I_R

Line I		*Line I_R*	
Velocity (km./sec.)	*Thickness* (km.)	*Velocity* (km./sec.)	*Thickness* (km.)
1·47 (water)	3·53	1·47 (water)	3·07
(2·0)	0·73	(2·0)	1·44
(3·6)	(1·0)	(3·6)	(1·0)
6·0	3·30	6·4	3·0
7·7	Unknown	8·3	Unknown

Average velocities, thicknesses and depths of the refractors are given in Table XIX. The thickness of the refractor with the true velocity of 6·2 km./sec. is a little less than the crustal thickness of 4 km. mapped by Ewing and Ewing (personal communication) in an adjacent area during 1958–59. The crustal thickness determined in this area is a little less than the average crustal thickness for oceanic areas.

TABLE XIX

AVERAGED RESULTS FOR LINES I AND I_R

Velocity (km./sec.)	*Thickness* (km.)	*Depth* (km.)
1·47 (water)	3·30	0
(2·0)	1·08	3·30
(3·6)	(1·0)	4·38
6·2	3·15	5·38
8·0	Unknown	8·53

12. *Lines J and J_R*

These two lines were shot in a north-east to south-west direction with the receiving station for line J at lat. 54°37′S., long. 39°58′W., and the receiving station for line J_R at lat. 54°20′S., long. 39°29′W. Water depths varied from 730 to 2,230 m. Because of the great difference in water depth at the two receiving stations, several depths below sea-level were used for the datum corrections. The refraction times for the 2·02 km./sec. velocity refractor determined on line J_R were corrected to the sea bottom, since this refractor composes the sea bed on this line. The arrivals from the 3·62 and 6·49 km./sec. velocity layers observed on line I_R were corrected to a datum of 1,445 m. below sea-level, whilst data from line I were corrected to a datum of 2,230 m. below sea-level. The following data were obtained from the travel-time graphs (Fig. 15):

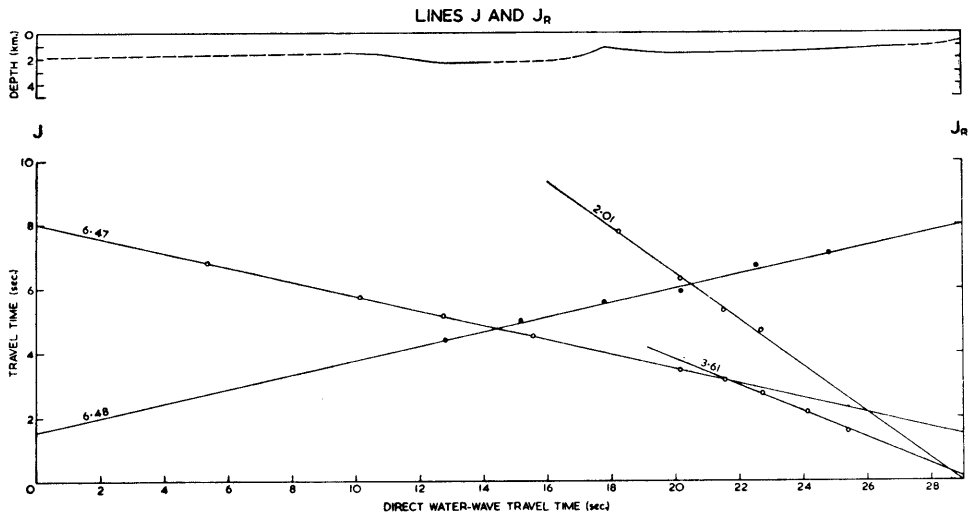

FIGURE 15
Travel times for lines J and J_R.

Line J $V_3 = 6{\cdot}50 \pm 0{\cdot}10$ km./sec. $t_3 = 1{\cdot}54 \pm 0{\cdot}53$ sec.
Line J_R $V_1 = 2{\cdot}02 \pm 0{\cdot}09$ km./sec. $t_1 = 0 \pm 0{\cdot}77$ sec.
$V_2 = 3{\cdot}62 \pm 0{\cdot}03$ km./sec. $t_2 = 0{\cdot}14 \pm 0{\cdot}28$ sec.
$V_3 = 6{\cdot}49 \pm 0{\cdot}12$ km./sec. $t_3 = 1{\cdot}27 \pm 0{\cdot}46$ sec.

The velocities of 2·02 and 3·62 km./sec. were not evident on line I. It was assumed that these refractors were also present on line I, and the thicknesses determined on line I_R, assuming that these refractors are horizontal, were also used on line I. The thicknesses of the refractors below the receiving stations are given in Table XX with the figures in brackets indicating assumed values of velocity and thickness.

TABLE XX

RESULTS FOR LINES J AND J_R

Line J		*Line J_R*	
Velocity (km./sec.)	*Thickness* (km.)	*Velocity* (km./sec.)	*Thickness* (km.)
1·46 (water)	1·90	1·46 (water)	0·73
(2·0)	0·67	2·0	0·87
(3·6)	(2·65)	3·6	2·65
6·5	Unknown	6·5	Unknown

The two apparent velocities determined for the V_3 refractor are both 6·5 km./sec., and they indicate that the refractor is horizontal. However, the depths of this refractor, determined on lines I and I_R from the intercept times, indicate that it is not horizontal. This ambiguity probably results from lines J and J_R not being exactly reversed. The velocities, mean thicknesses and depths of the refractors are given in Table XXI.

TABLE XXI

AVERAGED RESULTS FOR LINES J AND J_R

Velocity (km./sec.)	*Thickness* (km.)	*Depth* (km.)
1·46 (water)	1·31	0
2·0	0·77	1·31
3·6	2·65	2·08
6·5	Unknown	4·73

VI. DISCUSSION

1. *Current theories on the origin and evolution of the Scotia island arc*

The seismic refraction measurements require interpretation within the context of the geology of the surrounding land areas, if an understanding of the crustal geology of the Scotia Sea is to be gained. This approach is necessitated by the possible interdependence between the origin and evolution of the Scotia island arc and the crustal geology of the Scotia Sea. Both Matthews (1959) and Hawkes (1962) have discussed the nature, development and possible modes of formation of the Scotia island arc. Matthews has commented on the provenance of those sedimentary rocks occurring in the islands of the Scotia Ridge and he concluded that these islands probably represent areas with a crustal structure of a continental type. In particular, the sedimentary, intrusive and metamorphic rocks of South Georgia, Clerke Rocks, the South Orkney Islands and the Elephant and Clarence Islands group led Matthews to suggest that these islands could represent fragments of either a disrupted or partially submerged landmass. However, Griffiths and others (1964) have pointed out that the exposure of both shallow-water sediments and metamorphic rocks in the South Orkney Islands is inconsistent with the hypothesis of a sinking or sunken continental landmass.

Hawkes (1962) has suggested that the islands of the Scotia Ridge resulted from the fragmentation of a continental strip or land-bridge between the South American Andes and similar rocks of the Antarctic Peninsula during an eastward migration of the Pacific oceanic crust. He has cited the existence of Jurassic andesitic-rhyolitic volcanic rocks as evidence for the existence of a Mesozoic island arc and, in general, he envisaged the formation of volcanic island arcs at the eastward migrating junction between the oceanic and continental crusts in the region. Trendall (1959) also suggested the existence of a Mesozoic island arc to the south of South Georgia from an examination of current directions in the sediments of the Cumberland Bay Series which were mainly derived from volcanic material. Contrary to the suggestion of Matthews (1959), Hawkes (1962) believed that the crustal structure of the Scotia Sea is becoming more continental rather than more oceanic in character. Griffiths and others (1964) implied that the mode of formation of the Scotia Ridge suggested by Hawkes is inconsistent with its present length, and it could be that the north-north-west to south-south-west trend of the foliation axes in the basement rocks of the South Orkney Islands is also inconsistent with the positions of these islands in the reconstruction of the Palaeozoic orogenic belt between Tierra del Fuego and the Antarctic Peninsula (Hawkes, 1962, p. 88, fig. 1).

Other authors, whilst not proposing a comprehensive explanation of the origin and evolution of the Scotia Ridge, have generally believed that the Scotia Sea is bounded on the north and south by large transcurrent faults (Wilson, 1954; Heezen and Johnson, 1965). Most authors also agree that the general similarity of the volcanic rocks of the South Sandwich Islands to those of the Caribbean island arc, rather than to the volcanic rocks of the Andes, could indicate that the South Sandwich Islands group is a Recent formation which is not fundamentally related to the older islands of the Scotia Ridge (Hawkes, 1962; Heezen and Johnson, 1965).

The distribution of earthquake epicentres* (Gutenberg and Richter, 1954) reveals that there is little evidence for an active transcurrent fault zone along the northern limb of the Scotia Ridge between Tierra del Fuego and South Georgia. However, the epicentre data for the southern limb of the Scotia Ridge may provide more positive indications of transcurrent faulting, for which there is also some geological evidence in the South Orkney Islands (Adie, 1964).

2. *Summary of the results of seismic refraction investigations in the Scotia Sea*

Along those parts of the seismic profile between the South Orkney Islands and South Georgia, where sea depths are greater than 2 km. (Fig. 16), velocities of the crustal rocks vary from 5·7 to 6·2 km./sec. In similar, but shallower than typically oceanic sea depths, Ewing and Ewing (1959*a*) determined a velocity range of 5·7–6·3 km./sec. for the crustal rocks between Burdwood Bank and South Georgia. In both of these areas the crustal velocities and sea depths are less than those of typical oceanic areas, where average velocities of 6·5 km./sec. and depths of 5 km., respectively, are most common. The range of seismic velocities measured for the upper crustal layers in the eastern Scotia Sea is most probably indicative of acid crystalline rocks, whilst the velocity range of 7·4–7·6 km./sec., determined for the deeper layers in the southern part of the east Scotia Sea profile, is indicative of more basic rocks. The velocity of 8·0 km./sec., determined near the northern end of the seismic profile between the South Orkney Islands and South Georgia, is close to the defined mantle velocity of 8·1 km./sec. and it is similar to the velocities determined by Ewing and Ewing (1959*a*) in the western areas of the Scotia Sea and Drake Passage.

3. *Discussion of seismic results from other areas*

The crustal or velocity structure determined in the central parts of the seismic profile across the eastern Scotia Sea is comparable with the structure of the Mid-Atlantic Ridge determined by Le Pichon and others (1965). They have described a velocity structure of 5·8 km./sec. or lower, overlying a range of 7·2–7·6 km./sec. in the axial zone of the ridge, but the thickness of the lower-velocity or upper crustal layer appears to be greater in the central parts of the Scotia Sea. The East Pacific Rise has a sub-crustal velocity of 7·5–7·6 km./sec. (Raitt, 1964) but its crustal velocity of 6·5 km./sec. is that of a typically oceanic area and contrasts with velocities of 5·7–6·5 km./sec. recorded in the Scotia Sea. It is evident that mid-oceanic ridge or rise structures have a crustal structure which is different from that of typical oceanic areas, and that the central parts of the Scotia Sea seismic profile indicate a velocity structure which is similar in some respects to that of these ridges.

A lower or sub-crustal velocity (the description depends on the definition of the Earth's crust) of about 7·5 km./sec. has also been obtained on the continental rise off Newfoundland (Bentley and Worzel, 1956) and in the Norwegian Sea (Ewing and Ewing, 1959*b*). Velocities of 7·1–7·7 km./sec. have been determined by Officer and others (1959) in the Venezuelan Basin of the eastern Caribbean Sea, where sea depths vary between 4 and 5 km. It can therefore be concluded that lower or sub-crustal velocities of about 7·5 km./sec. often occur at the edges of continents, in the axial zones of the mid-oceanic ridges or rises, in seas where water depths are less than those typical of an oceanic region and in the vicinity of island arcs, such as the one surrounding the Caribbean Sea. However, because the velocity range of 7·1–7·7 km./sec. occurs in the almost typically oceanic depths of the Venezuelan Basin, it must be concluded that water depth alone cannot define the occurrence of this anomalous velocity range. Cook (1962) and others have described this velocity range in terms of a "mantle-crust mix" by suggesting that mixing of mantle and crustal rocks could explain the existence of these composite velocities.

The crustal structure of the Venezuelan Basin, where material with a velocity of 7·1–7·6 km./sec. occurs at a depth of about 10 km., can be compared with that of the south-eastern parts of the Scotia Sea, where velocities of 7·4–7·6 km./sec. occur at depths of 11–12 km. Heezen and Johnson (1965) have noted the similarities between the Scotia and Caribbean island arcs, and the seismic refraction investigations in the eastern parts of the Scotia Sea give additional emphasis to this similarity. In describing the results of seismic investigations in the Caribbean island arc, Officer and others (1957), and Ewing and others (1957) included the layer with a velocity of 7·1–7·6 km./sec. in the definition of the crust, and they concluded that the Caribbean island arc differs from the typical oceanic crust in having a wider range of crustal velocities and a thicker crust. They suggested that, if the structure of this region was originally

* A compilation of recent epicentre data for this region is at present being prepared by the British Antarctic Survey.

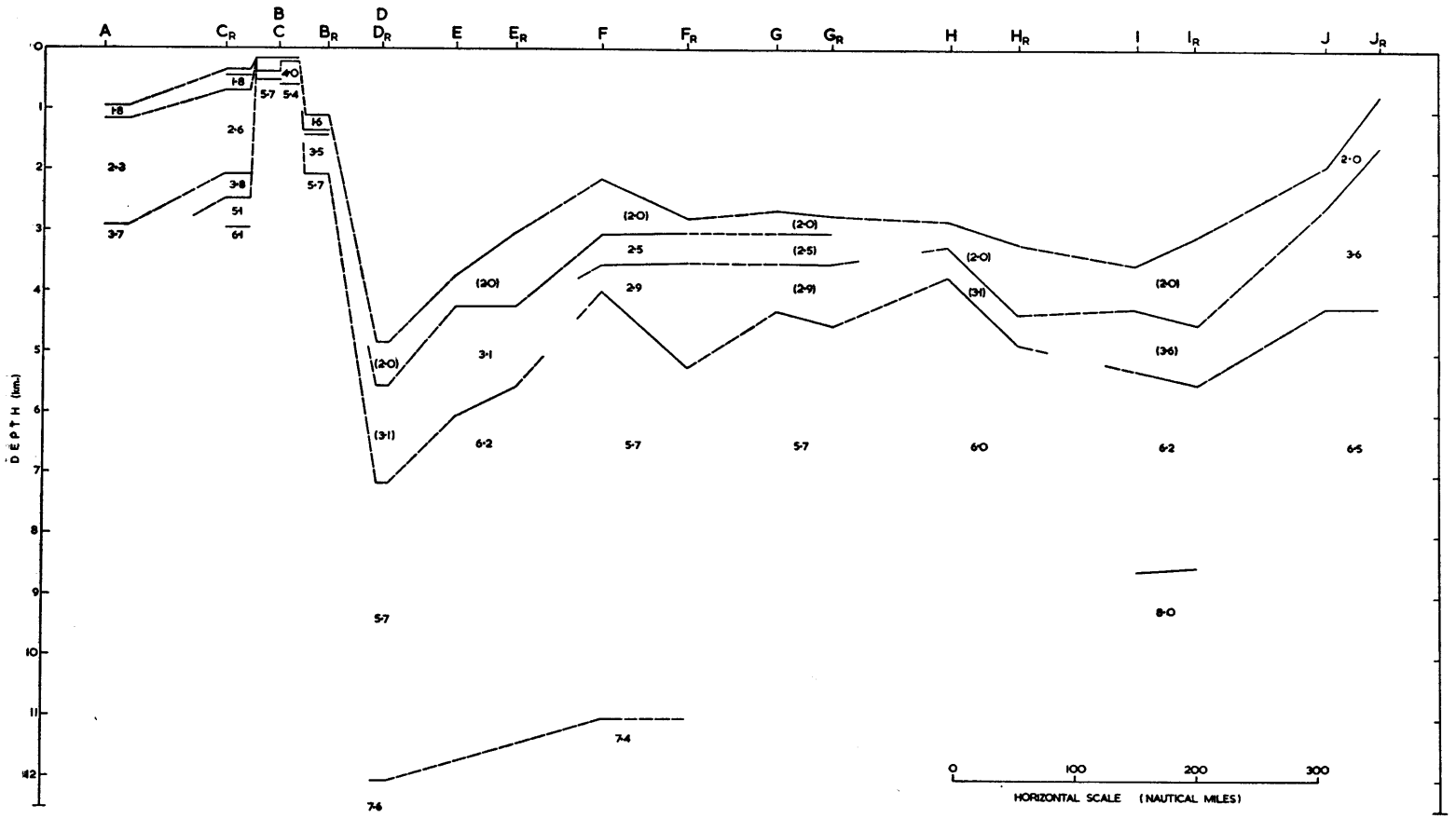

FIGURE 16

Crustal structure of the eastern Scotia Sea between the South Orkney Islands and South Georgia. The positions of the seismic lines are given in Fig. 1.

oceanic, then large amounts of crustal material must have been added to achieve the present structure. This addition would produce the observed features of the region which contrast markedly with those of typically oceanic areas. Thus the crust is thicker, the range in crustal velocities wider and the change from crustal to mantle velocities more gradual than in true oceanic areas. These characteristics are similar to those of the south-eastern Scotia Sea, and they may be indicative of a similar origin or evolution of the two regions. However, the inconsistencies in the theories of Matthews (1959) and Hawkes (1962) necessitate a further examination of the geology of the Scotia Sea region before an alternative theory on its origin and evolution can be proposed.

4. *Structure of the Falkland and Scotia Ridges*

Many authors have commented on the apparent continuation of the South American Andean mountain chain into the Antarctic Peninsula through the islands of the Scotia Ridge (Suess, 1909).

Harrington (1962) has provided information on the palaeogeographic development of South America. In an appendix to a paper by Ludwig, Ewing and Ewing (1965), Harrington has also given a comprehensive account of the structural framework of Magallanes Province. He has described four morphostructural units which can be distinguished in the southern parts of South America: the "Cordillera de la Costa of Chile, forming the outer row of islands of the Chilean Archipelago as far south as the Straits of Magellan"; the Patagonian Cordillera, which lies immediately to the east of the Coast Cordillera and extends across Tierra del Fuego to Staten Island; the Magellan Basin to the east of the Patagonian Cordillera; and the Deseado Massif, which is in the Rio Deseado—Rio Chico area. Each or all of these units could have an important bearing on the structure of the Falkland and Scotia Ridges, if they continue eastward into these ridges.

The physiographic diagram of the South Atlantic Ocean (Plate I) shows both the Falkland and north Scotia Ridges trending eastwards from southern Patagonia. The Falkland Ridge has a smooth low relief but the ridge between Burdwood Bank and South Georgia has a higher relief. Closer examination of Plate I reveals that Burdwood Bank may not form an integral part of the submarine north Scotia Ridge trending westwards from South Georgia. This ridge curves slightly northwards from South Georgia and it may skirt the eastern margins of Burdwood Bank in a north-east to south-west direction. There may be some magnetic evidence for the trend of this ridge near the eastern end of Burdwood Bank (Griffiths and others, 1964, fig. 40). Between the north Scotia Ridge and the Falkland Ridge there is a submarine trough (sometimes called the "Malvinas Chasm"), the depth of which may be as great as 3,000–4,000 m.

Baker (1922) has concluded that the (?) Precambrian schists and coarse pegmatites of Cape Meredith in the Falkland Islands are very similar to those found in the Cape Province of South Africa. It may be reasonable to suggest that the similar latitudes of the northern margins of the Deseado Massif and the Falkland Ridge (Plate I) could indicate that much of the Falkland Ridge might be substantially built on the essentially stable Precambrian rocks of the Deseado Massif. It is postulated here that the Falkland Ridge is a fragment of the ancient supercontinent of Gondwanaland; the essentially aseismic nature of this ridge, and possibly its smooth topography, would be compatible with such a structure. A velocity of 5·7 km./sec. has been given for the upper crustal layer of the Falkland Ridge (Ewing, Ludwig and Ewing, 1964) and a velocity range of 5·2–5·9 km./sec. has been given for the basement rocks underlying the Magellan Straits (Ludwig, Ewing and Ewing, 1965). The seismic velocities in these two areas are compatible with the suggested structure of the Falkland Ridge, although velocities alone cannot be regarded as positively diagnostic.

The crustal down-warping associated with Burdwood Bank (Woollard, 1960) can perhaps be correlated with that of the Magellan Basin (Ludwig, Ewing and Ewing, 1965, p. 1866, fig. 10). This basin has a depth of between 5 and 9 km., and the velocities of 4·0–4·3 km./sec. for the Cretaceous and Jurassic rocks within it are similar to the velocity of 4·5 km./sec. determined by Ewing and Ewing (Woollard, 1960) for the rocks beneath Burdwood Bank. Ewing and Ewing (1959*a*) have suggested that a velocity range of 4·0–4·5 km./sec. can probably be identified with "slightly metamorphosed shales and sandstones mixed with extrusive and intrusive igneous rocks". Suess (1909, p. 490) reported that volcanic rocks had been dredged from Burdwood Bank, and Macfadyen (1933) has also described dredged fragments of greenish shale and argillaceous limestone containing Upper Cretaceous and Lower Tertiary Foraminifera.

It could be that the Magellan Basin continues farther east than Burdwood Bank along the "Malvinas Chasm". Griffiths and others (1964) have constructed a map showing the character of magnetic anomalies in the Scotia Sea, and the area of *no magnetic anomaly* can be followed eastwards with some certainty as far as long. 50°W. The southern limit of this area would be expected to mark the approximate position of the southern margin of the eastward continuation of the Magellan Basin.

The Coast Cordillera of the Chilean Archipelago is composed of Precambrian metamorphic rocks, Cambrian to Permian rocks, Jurassic marine deposits and some shallow-water Cretaceous sediments (Harrington, 1962; Ludwig, Ewing and Ewing, 1965). It is probable that this cordillera was a geosyncline which was uplifted and folded in late Palaeozoic to Triassic times before subsiding to comparatively shallow depths during the Jurassic or early Cretaceous. This cordillera formed a western threshold to the younger Patagonian-Fuegan geosyncline and both were uplifted during the Upper Cretaceous. It is suggested that the submarine ridge, which extends from the eastern margins of Burdwood Bank to South Georgia, is an eastward continuation of the cordilleran system of Tierra del Fuego. If this were so, then it would be expected that the seismicity of this submarine ridge would be similar to that of the Andes in southern Patagonia. Sykes (1963) has observed that the seismicity associated with the Andes shows a marked decrease in frequency where it is intersected at lat. 47°S. by the west Chile submarine ridge. Thus, the essentially aseismic nature of the north Scotia Ridge, between Burdwood Bank and South Georgia (Fig. 1), is consistent with the low level of seismicity in Tierra del Fuego.

There is no great thickness of post-Aptian sediments in the Coast Cordillera of Chile, or in the islands of the Scotia Ridge and the Antarctic Peninsula. The Aptian sediments of South Georgia and the shallow-water conglomerates of the South Orkney Islands have an age similar to that of the shallow-water sediments of the Coast Cordillera. It has been suggested that the geosyncline in which the Greywacke-Shale Series of the South Orkney Islands, the Trinity Peninsula Series of Graham Land and the Sandebugten Series of South Georgia were deposited extended between South America and Graham Land in (?) Carboniferous times (Adie, 1964). The provenance of these sediments demands a derivation from a landmass of considerable size (Matthews, 1959) and it is suggested that they were deposited in an epicontinental geosyncline associated with the ancient continent of Gondwanaland. The Mesozoic volcanic archipelago, which Trendall (1959) has postulated as a source for the Cumberland Bay Series, could have been associated with the period of intense vulcanicity offshore from Colombia to Tierra del Fuego, which was responsible for the marine deposition of vast quantities of flow lavas and tuffs in South America (Harrington, 1962). However, it is clear that during Aptian times, when the upper parts of the Cumberland Bay Series were deposited, there was little vulcanicity in South America. Moreover, the Aptian volcanic rocks of South Georgia are largely spilitic, whereas the Upper Jurassic volcanic rocks of the west coast of South America, the Antarctic Peninsula and the South Shetland Islands are andesitic to rhyolitic in composition.

5. *Origin and evolution of the Scotia Ridge*

The relationships between South America, southern Africa, India, Australia and Antarctica, as parts of the supercontinent of Gondwanaland before its disruption at the end of the Jurassic, or even the early Cretaceous, have been discussed by du Toit (1937), King (1958) and Martin (1961), among others. King and Downard (1964) and Adie (1965) have investigated the importance of Antarctica in relation to continental drift and, although King and Downard have discussed the break-up of the orogenic belt of western Antarctica with some reference to the geophysical investigations of Bentley and others (1960), no detailed study of the place of the whole Scotia Ridge during the drift of Antarctica has been attempted.

If the continental shelves of South America and southern Africa are fitted together in the reconstruction proposed by King (1958), then the Cape Province of South Africa and the Falkland Ridge are adjacent to one another. During the late Palaeozoic the Coast Pre-cordillera or geosyncline of Chile continued eastwards along the southern side of the Falkland Ridge, through South Georgia and the South Orkney Islands, to the Antarctic Peninsula. The vigorous folding of the Sandebugten Series of South Georgia, the Greywacke-Shale Series of the South Orkney Islands and the Trinity Peninsula Series of the Antarctic Peninsula occurred during the early Mesozoic, before the flat-lying Middle Jurassic sediments of the north-east Antarctic Peninsula and the shallow-water Cretaceous sediments of Chile and the Scotia Ridge were deposited. The age of the folding of the Greywacke-Shale Series in the South Orkney Islands

is corroborated by the K/A date (183 m. yr.) of the last major orogeny which affected the Basement Complex in this area (Miller, 1960).

Shortly after the late Jurassic period of offshore vulcanicity from Chile to the Antarctic Peninsula along the length of the early Mesozoic cordillera, the incipient Mid-Atlantic Ridge began to develop between the continental shelves of South America and southern Africa, and between the Falkland Ridge and the Cape Province. The disruption of Gondwanaland was completed by the mid-Cretaceous, as Antarctica and South America drifted relatively south and westwards from southern Africa (King, 1958). The Falkland Ridge, which is an integral part of the South American continental block, and that part of the early Mesozoic cordillera between Tierra del Fuego and South Georgia remained in their same positions relative to South America. Further south-westward drift of Antarctica caused the rupture of this cordillera between the South Orkney Islands and South Georgia. The continental block of Antarctica, the Antarctic Peninsula and the South Orkney Islands may have undergone a rotation of about 90° before the cordillera was again broken and the South Orkney Islands were left behind as the Antarctic Peninsula approached its present position. The fragmentation of the early Mesozoic cordillera between the South Orkney Islands and the Antarctic Peninsula is substantiated by the directions of the foliation axes in the Basement Complex of the Elephant and Clarence Islands group and the South Orkney Islands, where trends of approximately east-north-east to west-south-west and north-north-west to south-south-east, respectively, have been observed (Tyrrell, 1945; Matthews, 1959). These breaks in the early Mesozoic cordillera may also be associated with the discontinuity in the western Antarctic orogenic belt between the Antarctic Peninsula—Sentinel Range segment and the Kohler Range (Bentley and others, 1960). The results of palaeomagnetic investigations by Blundell and Stephenson (1959) in the Weddell Sea sector of Antarctica suggest that South America and Antarctica drifted closer together during the Mesozoic, and that Antarctica had already reached its present position by the beginning of the "Andean orogeny",* during the late Cretaceous or early Tertiary.

The "Andean orogeny" uplifted the Patagonian-Fuegan Cordillera of South America and was responsible for large-scale block-faulting and uplift in the Antarctic Peninsula. It has resulted in little or no folding in South America (Gerth, 1960), or in the Antarctic Peninsula, and probably only minor folding in South Georgia, where it has been shown (p. 40) that the major folding is early Mesozoic in age. In the South Orkney Islands the minor east—west folding (Matthews, 1959), which is probably late Cretaceous–early Tertiary, did not modify the K/A date of the last *major* orogeny in the area. The continuity of the early Mesozoic cordillera was broken between South Georgia and the South Orkney Islands, and it is proposed that the adjacent or co-linear "Andean orogeny" of South America and the Antarctic Peninsula maintained its continuity by the development of a submarine volcanic arc, which lay to the west of the South Sandwich Islands group and extended from South Georgia to the South Orkney Islands (p. 42). This volcanic arc might be compared with the primary volcanic mountain arcs of the Andes (Wilson, 1954), and the absence of exposures of the Andean Intrusive Suite in the South Orkney Islands could be explained by the fragmentation of the Palaeozoic geosynclincal belt in that area. This proposal need not be contradicted by the exposure of the Andean Intrusive Suite in south-eastern South Georgia, since the Palaeozoic geosynclinal belt was probably continuous between this area and Tierra del Fuego.

The volcanic rocks of the South Sandwich Islands are not related to the volcanic rocks of the Andes. Tyrrell (1945) has observed that they have an andesitic to basaltic composition, which is similar to that of the volcanic rocks of the Caribbean island arc. The position of the South Sandwich Islands may be controlled by the zone of crustal weakness left between South Georgia and the South Orkney Islands by the fragmentation of the early Mesozoic cordillera.

6. *Relationship between the results of the seismic refraction survey and the evolution of the Scotia Ridge*

It has been argued above that South Georgia and the South Orkney Islands are among those islands of the Scotia Ridge which are fragments of an early Mesozoic cordillera that at one time extended from Tierra del Fuego to the Antarctic Peninsula. The seismic velocities of about 3·6 and 4·0 km./sec., determined in the areas of South Georgia and the South Orkney Islands, respectively, may be those of the Upper Palaeozoic sediments in these two areas. The seismic velocities (5·1–5·9 km./sec.) of the

* The term "Andean orogeny" has the merits of common usage and brevity, but its use is not strictly correct, since there is little evidence of compression in the "Andean orogenic belt" (Gerth, 1960).

deeper refractors beneath the South Orkney Islands shelf are similar to those (5·2–5·9 km./sec.) determined for the basement rocks in the Magellan Basin area of Tierra del Fuego. The exposure of Basement Complex metamorphic rocks in the South Orkney Islands justifies the association of the velocity range of 5·1–5·7 km./sec. with these rocks.

The southern part of the seismic refraction profile across the Scotia Sea may be located over the group of submarine ridges which extend in a north-easterly direction from just north of the South Orkney Islands. It has been suggested that a submarine volcanic arc may extend from South Georgia to the South Orkney Islands as part of the continuous "Andean orogenic belt", and it could therefore be significant that velocities of 7·4–7·6 and 7·5 km./sec. have been determined to the north-east of the South Orkney Islands and to the south of South Georgia (Ewing and Ewing, 1959*a*), respectively, whilst an almost typical mantle velocity of 8·0 km./sec. has been determined to the west of South Georgia (Fig. 16).

In discussing the velocities of about 7·4 km./sec. determined in the Venezuelan Basin of the Caribbean Sea, Ewing and others (1957) have postulated that they may be indicative of a crust which has been injected by a low-velocity primary differentiate that has migrated from deep within the mantle, and which is in the process of changing from an oceanic to a continental character. This theory could be directly applicable to the crustal structure determined at the southern end of the seismic profile across the Scotia Sea, and the low-velocity primary differentiate in this case may be identified with the volcanic rocks of the submarine arc between South Georgia and the South Orkney Islands.

VII. ACKNOWLEDGEMENTS

THE author wishes to acknowledge the comprehensive facilities provided by Sir Vivian Fuchs, Director of the British Antarctic Survey, and the helpful co-operation of Captain D. Turnbull (R.R.S. *Shackleton*) and Captain R. H. Graham, M.V.O., D.S.C., R.N. (H.M.S. *Protector*) during the survey operations. The author is also grateful to Dr. R. J. Adie for his criticism of the geological aspects and presentation of this report, to Professor D. H. Griffiths for his helpful supervision and to Professor F. W. Shotton for providing the laboratory facilities.

VIII. REFERENCES

ADIE, R. J. 1957*a*. Geological Research in Graham Land. *Advanc. Sci., Lond.*, No. 53, 454–60.

————. 1957*b*. The Petrology of Graham Land: III. Metamorphic Rocks of the Trinity Peninsula Series. *Falkland Islands Dependencies Survey Scientific Reports*, No. 20, 26 pp.

————. 1958. Geological Investigations in the Falkland Islands Dependencies since 1940. *Polar Rec.*, **9**, No. 58, 3–17.

————. 1962. The Geology of Antarctica. (*In* WEXLER, H., RUBIN, M. J. *and* J. E. CASKEY, *ed. Antarctic Research: the Matthew Fontaine Maury Memorial Symposium.* Washington, D.C., American Geophysical Union, 26–39.) [Geophysical Monograph No. 7.]

————. 1964. Geological History. (*In* PRIESTLEY, R. E., ADIE, R. J. *and* G. DE Q. ROBIN, *ed. Antarctic Research.* London, Butterworth and Co. (Publishers) Ltd., 118–62.)

————. 1965. Antarctic Geology and Continental Drift. *Sci. J., Lond.*, **1**, No. 6, 65–73.

ARONS, A. B. *and* D. R. YENNIE. 1950. Phase Distortion of Acoustic Pulses Obliquely Reflected from a Medium of Higher Sound Velocity. *J. acoust. Soc. Am.*, **22**, 231–37.

BAKER, H. A. 1922. *Final Report on Geological Investigations in the Falkland Islands, 1920-1922.* Port Stanley, Government Printer.

BARTH, T. F. W. *and* P. HOLMSEN. 1939. Rocks from the Antarctandes and the Southern Antilles. Being a Description of Rock Samples Collected by Olaf Holtedahl 1927–1928, and a Discussion of Their Mode of Origin. *Scient. Results Norw. Antarct. Exped.*, No. 18, 64 pp.

BENTLEY, C. R. *and* J. L. WORZEL. 1956. Geophysical Investigations in the Emerged and Submerged Atlantic Coastal Plain. Part X. Continental Slope and Continental Rise South of the Grand Banks. *Bull. geol. Soc. Am.*, **67**, No. 1, 1–18.

————., CRARY, A. P., OSTENSO, N. A. *and* E. C. THIEL. 1960. Structure of West Antarctica. *Science, N.Y.*, **131**, No. 3394, 131–36.

BLUNDELL, D. J. *and* P. J. STEPHENSON. 1959. Palaeomagnetism of Some Dolerite Intrusions from the Theron Mountains and Whichaway Nunataks, Antarctica. *Nature, Lond.*, **184**, No. 4702, 1860.

COOK, K. L. 1962. The Problem of the Mantle-crust Mix: Lateral Inhomogeneity in the Uppermost Part of the Earth's Mantle. (*In* LANDSBERG, H. E. *and* J. VAN MIEGHEM, *ed. Advances in Geophysics*, **9**. New York and London, Academic Press, 295–360.)

COX, M. J. G. 1964. Seismic Refraction Measurements in Bransfield Strait. *British Antarctic Survey Bulletin*, No. 4, 1–12.

DIX, C. H. 1952. *Seismic Prospecting for Oil.* New York, Harper and Brothers.

DOBRIN, M. B. 1960. *Introduction to Geophysical Prospecting.* 2nd edition. New York, Toronto, London, McGraw-Hill Book Company, Inc.

DRAKE, C. L., EWING, M. *and* G. H. SUTTON. 1959. Continental Margins and Geosynclines: the East Coast of North America North of Cape Hatteras. (*In* AHRENS, L. H., PRESS, F., RANKAMA, K. *and* S. K. RUNCORN, *ed. Physics and Chemistry of the Earth*, **3**. London, New York and Paris, Pergamon Press, 110–98.)

DYK, K. *and* O. W. SWAINSON. 1953. The Velocity and Ray Paths of Sound Waves in Deep Sea Water. *Geophysics*, **18**, No. 1, 75–103.

EWING, J. I. 1963. Elementary Theory of Seismic Refraction and Reflection Measurements. (*In* HILL, M. N., *ed. The Sea. Ideas and Observations on Progress in the Study of the Seas. Vol. 3. The Earth Beneath the Sea: History.* New York, London, Interscience Publishers, 3–19.)

———. *and* M. EWING. 1959*a*. Seismic Refraction Measurements in the Scotia Sea and South Sandwich Island Arc. (*In* SEARS, M., *ed. International Oceanographic Congress Preprints.* Washington, D.C., American Association for the Advancement of Science, 22–23.)

———. *and* ———. 1959*b*. Seismic-refraction Measurements in the Atlantic Ocean Basins, in the Mediterranean Sea, on the Mid-Atlantic Ridge, and in the Norwegian Sea. *Bull. geol. Soc. Am.*, **70**, No. 3, 291–317.

———., OFFICER, C. B., JOHNSON, H. R. *and* R. S. EDWARDS. 1957. Geophysical Investigations in the Eastern Caribbean: Trinidad Shelf, Tobago Trough, Barbados Ridge, Atlantic Ocean. *Bull. geol. Soc. Am.*, **68**, No. 7, 897–912.

EWING, M., LUDWIG, W. J. *and* J. I. EWING. 1964. Sediment Distribution in the Oceans: the Argentine Basin. *J. geophys. Res.*, **69**, No. 10, 2003–32.

FRY, J. C. *and* R. W. RAITT. 1961. Sound Velocities at the Surface of Deep Sea Sediments. *J. geophys. Res.*, **66**, No. 2, 589–97.

GERTH, H. 1960. Die Entwicklung der Orogene der südamerikanischen Kordillere während des Mesozoikums. *Geol. Rdsch.*, **50**, 619–30.

GORDON, W. T. 1930. A Note on *Dadoxylon* (*Araucarioxylon*) from the Bay of Isles. (*In Report on the Geological Collections Made during the Voyage of the "Quest" on the Shackleton—Rowett Expedition to the South Atlantic and Weddell Sea in 1921-1922.* London, British Museum (Nat. Hist.), 24–27.)

GRIFFITHS, D. H., RIDDIHOUGH, R. P., CAMERON, H. A. D. *and* P. KENNETT. 1964. Geophysical Investigation of the Scotia Arc. *British Antarctic Survey Scientific Reports*, No. 46, 43 pp.

GUTENBERG, B. *and* C. F. RICHTER. 1954. *Seismicity of the Earth and Associated Phenomena.* 2nd edition. Princeton, Princeton University Press.

HARRINGTON, H. J. 1962. Palaeogeographic Development of South America. *Bull. Am. Ass. Petrol. Geol.*, **46**, No. 10, 1773–814.

HAWKES, D. D. 1962. The Structure of the Scotia Arc. *Geol. Mag.*, **99**, No. 1, 85–91.

HEEZEN, B. C. *and* G. L. JOHNSON. 1965. The South Sandwich Trench. *Deep Sea Res.*, **12**, No. 2, 185–97.

HILL, M. N. 1952. Seismic Refraction Shooting in an Area of the Eastern Atlantic. *Phil. Trans. R. Soc.*, Ser. A, **244**, No. 890, 561–94.

HOLTEDAHL, O. 1929. On the Geology and Physiography of Some Antarctic and Sub-Antarctic Islands. *Scient. Results Norw. Antarct. Exped.*, No. 3, 172 pp.

HORTON, J. W. 1957. *Fundamentals of Sonar.* Annapolis, Maryland, U.S. Naval Institute.

KATZ, S. *and* M. EWING. 1956. Seismic-refraction Measurements in the Atlantic Ocean. Part VII: Atlantic Ocean Basin, West of Bermuda. *Bull. geol. Soc. Am.*, **67**, No. 4, 475–509.

KING, L. C. 1958. Basic Palaeogeography of Gondwanaland during the Late Palaeozoic and Mesozoic Eras. *Q. Jl geol. Soc. Lond.*, **114**, Pt. 1, No. 453, 47–77.

———. *and* T. W. DOWNARD. 1964. Importance of Antarctica in the Hypothesis of Continental Drift. (*In* ADIE, R. J., *ed. Antarctic Geology.* Amsterdam, North-Holland Publishing Company, 727–35.)

LUDWIG, W. J., EWING, J. I. *and* M. EWING. 1965. Seismic-refraction Measurements in the Magellan Straits. *J. geophys. Res.*, **70**, No. 8, 1855–76.

MACFADYEN, W. A. 1933. Fossil Foraminifera from the Burdwood Bank and Their Geological Significance. '*Discovery*' *Rep.*, **7**, 1–16.

MARTIN, H. 1961. The Hypothesis of Continental Drift in the Light of Recent Advances of Geological Knowledge in Brazil and South West Africa. (Alex. L. du Toit Memorial Lectures, No. 7.) *Trans. Proc. geol. Soc. S. Afr.*, **64** (annexure), 1–47.

MATTHEWS, D. H. 1959. Aspects of the Geology of the Scotia Arc. *Geol. Mag.*, **96**, No. 6, 425–41.

MATTHEWS, D. J. 1939. *Tables of the Velocity of Sound in Pure Water and Sea Water for Use in Echo-sounding and Sound-ranging.* 2nd edition. London, His Majesty's Stationery Office. [Admiralty Hydrographic Department, H.D.282.]

MILLER, J. A. 1960. Potassium-argon Ages of Some Rocks from the South Atlantic. *Nature, Lond.*, **187**, No. 4742, 1019–20.

NETTLETON, L. L. 1940. *Geophysical Prospecting for Oil.* New York and London, McGraw-Hill Book Company, Inc.

OFFICER, C. B., EWING, J. I., EDWARDS, R. S. *and* H. R. JOHNSON. 1957. Geophysical Investigations in the Eastern Caribbean: Venezuelan Basin, Antilles Island Arc, and Puerto Rico Trench. *Bull. geol. Soc. Am.*, **68**, No. 3, 359–78.

———., ———., HENNION, J. F., HARKRIDER, D. G. *and* D. E. MILLER. 1959. Geophysical Investigations in the Eastern Caribbean: Summary of 1955 and 1956 Cruises. (*In* AHRENS, L. H., PRESS, F., RANKAMA, K. *and* S. K. RUNCORN, *ed. Physics and Chemistry of the Earth*, **3**. London, New York and Paris, Pergamon Press, 17–109.)

PICHON, X. LE, HOUTZ, R. E., DRAKE, C. L. *and* J. E. NAFE. 1965. Crustal Structure of the Mid-ocean Ridges. 1. Seismic Refraction Measurements. *J. geophys. Res.*, **70**, No. 2, 319–39.

RAITT, R. W. 1964. Geophysics of the South Pacific. (*In* ODISHAW, H., *ed. Research in Geophysics. Vol. 2. Solid Earth and Interface Phenomena.* Cambridge, Massachusetts, The Massachusetts Institute of Technology Press, 223–41.)

RAYLEIGH, *Baron.* 1945. *The Theory of Sound*, **2**. 2nd edition. New York, Dover Publications.

SHOR, G. G. 1963. Refraction and Reflection Techniques and Procedures. (*In* HILL, M. N., *ed. The Sea. Ideas and Observations on Progress in the Study of the Seas. Vol. 3. The Earth Beneath the Sea: History*, New York, London, Interscience Publishers, 20–37.)

SUESS, E. 1909. *Das Antlitz der Erde. Vol. III ii.* Leipzig, G. Freytag; Wien, F. Tempsky.

SYKES, L. R. 1963. Seismicity of the South Pacific Ocean. *J. geophys. Res.*, **68**, No. 21, 5999–6006.

TILLEY, C. E. 1935. Report on Rocks from the South Orkney Islands. '*Discovery*' *Rep.*, **10**, 383–90.

TOIT, A. L. DU. 1937. *Our Wandering Continents.* Edinburgh, Oliver and Boyd.

TRENDALL, A. F. 1953. The Geology of South Georgia: I. *Falkland Islands Dependencies Survey Scientific Reports*, No. 7, 26 pp.

———. 1959. The Geology of South Georgia: II. *Falkland Islands Dependencies Survey Scientific Reports*, No. 19, 48 pp.

TYRRELL, G. W. 1945. Report on Rocks from West Antarctica and the Scotia Arc. '*Discovery*' *Rep.*, **23**, 37–102.

WILSON, J. T. 1954. The Development and Structure of the Crust. (*In* KUIPER, G. P., *ed. The Solar System: II. The Earth as a Planet.* Chicago, University of Chicago Press, 138–214.)

WOOD, A. 1940. *Acoustics.* London and Glasgow, Blackie and Son Limited.

WOOLLARD, G. P. 1960. Seismic Crustal Studies during the IGY. Part I: Marine Program. *Trans. Am. geophys. Un.*, **41**, No. 1, 107–13. [*IGY Bull.*, No. 33, 1–7.]

PLATE I

The physiography of the Scotia Sea and the Scotia and Falkland Ridges. (From "Physiographic diagram of the South Atlantic Ocean, the Caribbean Sea, the Scotia Sea, and the eastern margin of the South Pacific Ocean" (HEEZEN, B. C. *and* M. THARP. 1961. Geological Society of America). Reproduced by permission of the authors and the Geological Society of America.)

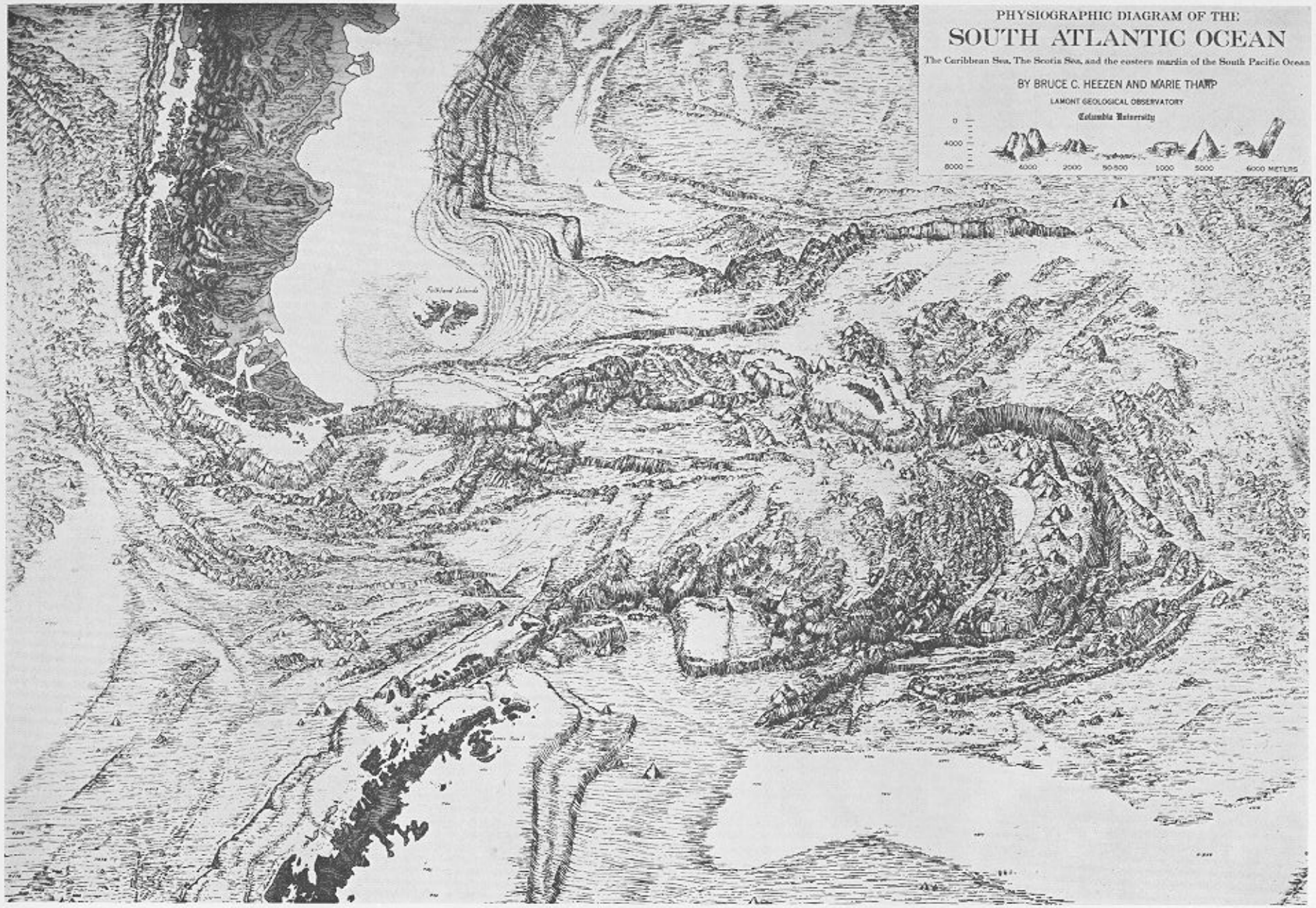
PHYSIOGRAPHIC DIAGRAM OF THE
SOUTH ATLANTIC OCEAN
The Caribbean Sea, The Scotia Sea, and the eastern margin of the South Pacific Ocean
BY BRUCE C. HEEZEN AND MARIE THARP
LAMONT GEOLOGICAL OBSERVATORY
Columbia University
0
4000
8000
6000
2000
50-500
1000
5000
6000 METERS

PLATE I

PLATE II

Part of a seismogram recorded on line E (Fig. 1), showing the water wave and the first- and second-order reflection events.

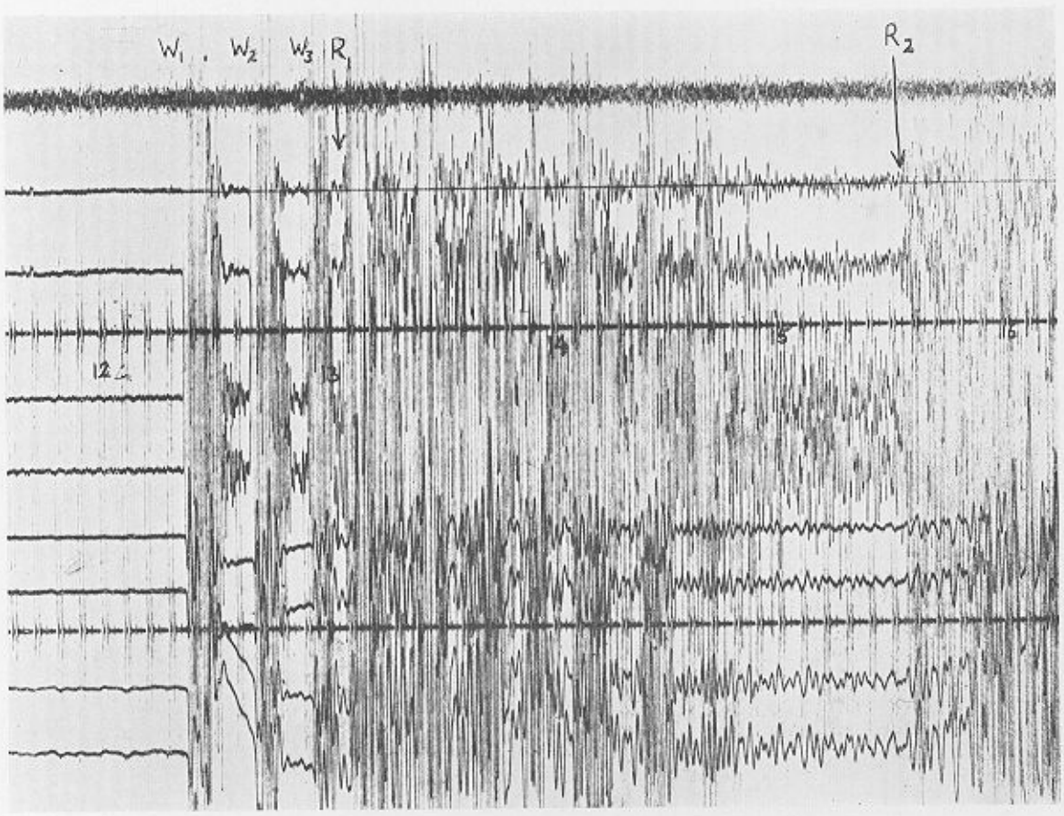
W1
W2
W3
R1
R2